JYVÄSKYLÄN YLIOPISTO
UNIVERSITY OF JYVÄSKYLÄ

Characterization of a self-seeded grating-based Ti:sapphire laser

Master's Thesis

Author: Efstathios Giannopoulos
Supervisors: Prof. Iain Moore, Dr. Mikael Reponen
1 MAY 2019

Abstract

Giannopoulos, Efstathios

Characterization of a self-seeded grating-based Ti:sapphire laser

Master's Thesis

Department of Physics, University of Jyväskylä, Finland, 2019, pages 40

The work presented in this master thesis focuses on the upgrade of the grating-based Ti:sapphire laser system, which is located in IGISOL facility in the University of Jyväskylä, Finland. The classic grating Ti:sapphire laser is upgraded to the self-seeded grating-based Ti:sapphire laser with the addition of a partially reflecting mirror. This upgrading was done in order to increase the output power of the cavity. Then, the combination between the self-seeded grating-based Ti:sapphire laser and the existing three Ti:sapphire systems of laboratory are used for the search of auto-ionizing states in elements, such as silver, as well as for the saturation measurements and the delay curve.

Keywords: Ti:sapphire, saturation, Rydberg series, Silver.

Acknowledgements

First and foremost, I would like to thank my professor and supervisor Iain Moore for giving me the chance to be a part of his team. From the beginning till the end, he encouraged me and I really thank him for being patient, giving me guidance and helping me to improve. Furthermore, I am particularly grateful to him for giving me the opportunity through the recommendation letter to be admitted to the CERN summer school of 2017.

In the same time, I would like to express my heartfelt thanks to my co-supervisor Dr. Mikael Reponen for the invaluable assistance that he offered me to carry out the work presented in this thesis. He was there for me at any difficulty that I dealt with during my thesis. Many thanks for his assistance in our project and spending time with me.

I deeply thank both supervisors for their extending compassion and flexibility when I needed it.

A great thank to Dr. Sami Räsänen for all the long discussions that we done during the lectures of master thesis seminar. He was really helpful and kind. In addition, I would like particularly thank the secretary Mrs. Minttu Haapaniemi for her kind help and giving me all the requested information, in every application that had to be filled.

A big thanks goes to my family for their support and trust to me during the last 2,5 years. A special mention goes to my friend Dr. Phillipos Papadakis for the priceless advices that he offered me during my master. Last but not least, I want to thank my girlfriend Penny from the bottom of my heart, for her support, trust and love during my "journey".

Contents

1. Introduction

Many radioactive beam facilities use the laser ion source in order to improve the ionization efficiency as well as the selectivity [1].

Wide range wavelength tunability is important for laser spectroscopy, as it enables optical research into unknown atomic systems. There is a shortage of spectroscopic information in the area of higher – lying excited states region for a large number of elements. This fact becomes even more severe for heavier elements that consist of a complicated electronic structure. As a consequence, the only viable way to get spectroscopic data is by direct measurement.

The standard pulsed Ti:sapphire laser systems are not so versatile for tuning, and in many cases, they lead to mode – hops and strong output power fluctuations. This is due to the use optical elements during the scanning of the wavelength, like birefringent filter and etalon. If the laser is utilized for spectroscopy, these problems have to be eliminated. A more convenient way to realize mode – hop free wavelength tunability is to utilize a grating. The use of a grating for selecting wavelength, permits scanning for long wavelength ranges [2]. However, the fundamental output power of a grating-based Ti:sapphire laser is much lower than the standard pulsed Ti:sapphire, which results, for example, in low second harmonic generation efficiency and low ionization efficiency. Based on recent developments [3], a self-seeded grating laser is built to greatly increase the fundamental output power, while preserving the GHz - range linewidth.

This thesis consists of six chapters. The Chapter 1 is the Introduction – Motivation. The Chapter 2 includes the necessary theoretical background for understanding the subject of the thesis; namely, the theory of the basic principles of the laser operation and the laser properties. In addition, the diffraction grating, the theory of the Ti:sapphire laser as well as the atom – light interaction and the resonance ionization spectroscopy are all presented. The Chapter 3 contains the experimental setup. It describes the tools, which are used to fulfil this project, such as the properties of the pump lasers, the optical table layout as well as the electronic setup.

The Chapter 4 and 5 present the experimental analysis – results. The Chapter 4 refers to the setup of a self-seeded grating-based Ti:sapphire laser and its upgrading. The combination between the self-seeded grating-based Ti:sapphire laser and the existing three Ti:sapphire systems of laboratory is discussed in Chapter 5.

In the Chapter 6, the summary and the future projects are discussed.

2. Theoretical background

2.1. Laser

The word LASER comes from the initials of the words **L**ight **A**mplification by **S**timulated **E**mission of **R**adiation.

2.1.1. Absorption, spontaneous and stimulated emission

Assuming that it is used a simplified model of two energy levels of an atom, with energies E_1 (ground state) and E_2 (excited state) where $E_1 < E_2$ (Fig. 2.1). If the atom is in the excited state and because $E_2 > E_1$, the atom will tend to decay to the ground state and releases energy equal to the difference between $E_2 - E_1$. If the energy is emitted in the form of an electromagnetic (EM) wave, the process is called *spontaneous emission*, and is characterized by the emission of a photon energy $hv_0 = E_2 - E_1$ (Fig. 2.1.a). The transition to the ground state can also be made with a non-radiative way, for example by molecular collisions, and in this case the process is called non-radiative decay [4].

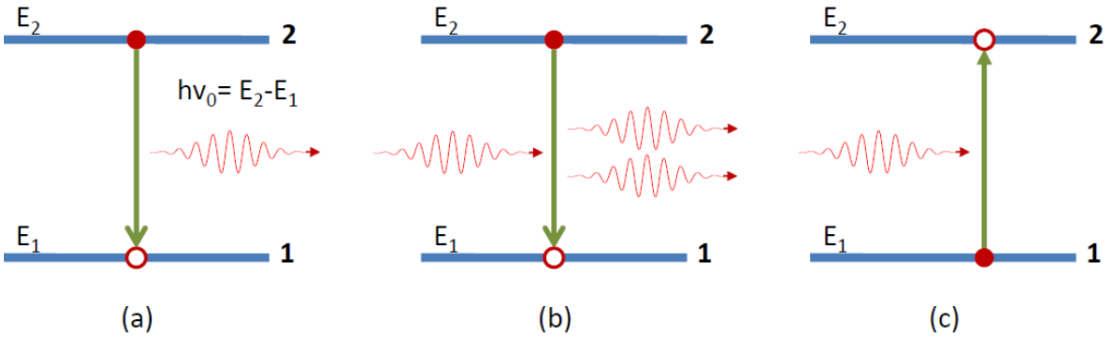

Figure 2.1. (a) Spontaneous emission, (b) Stimulated emission and (c) Absorption.

Supposing now that the atom is in the excited state and an EM frequency wave $v = v_0$ disrupts it. Because the EM wave has the same frequency as the atomic frequency, there is a non-zero probability that the atom goes to the ground state by emitting a photon $hv_0 = E_2 - E_1$, due to the disturbing EM field (Fig. 2.1.b). The phenomenon is called *stimulated emission*.

It is worth to emphasize to the essential difference between stimulated and spontaneous emission. During the stimulated emission, the atoms emit EM waves which are in phase with the incident EM field and they are emitted at the same direction. In contrast, in the spontaneous emission, the emitted EM waves have no definite phase in relation to the incident EM field and are emitted at any direction.

Assuming now, that the atom is at the ground state and an EM frequency wave $v = v_0$ disrupts it. Thus, there is a non-zero probability that the atom goes from the ground state to the excited state, increasing its energy at $E_2 - E_1$ because of disrupting EM field (Fig. 2.1.c). The phenomenon is called *absorption*.

To understand the above processes, the number N_i is introduced. The N_i is the number of atoms (or molecules) per unit of volume in the E_i state and is called population of the state i.

Spontaneous emission**:** The decay rate of the E_2 population is proportional to the N_2 population.

$$(\frac{dN_2}{dt})_{SP} = -AN_2. \quad (2.1)$$

The coefficient A is a positive constant and is called *Einstein coefficient A* or *rate* of spontaneous emission. It depends only on the particular transition. The $\tau_{SP} = {}^{1}/_{A}$ is the lifetime of spontaneous emission.

Non-radiative decay**:**

$$(\frac{dN_2}{dt})_{NR} = -{}^{N_2}/_{\tau_{NR}}. \quad (2.2)$$

The $\tau_{NR} = {}^{1}/_{A}$ is the lifetime of the non-radiative decay and depends not only on that transition, but also on the surrounding environment.

Stimulated emission**:**

$$(\frac{dN_2}{dt})_{ST} = -W_{21}N_2. \quad (2.3)$$

The coefficient W_{21} is the rate of stimulated emission, with dimensions of inverse time, and depends both on the specific transition and on the intensity of the incident wave.

Absorption:

$$(\frac{dN_2}{dt})_{A} = -W_{12}N_1. \quad (2.4)$$

The coefficient W_{12} is the rate of absorption and depends not only on that transition, but also on the intensity of the incident wave.

Considering plane waves for the incident wave are used, the following equations are applied:

$$W_{12} = \sigma_{12}F. \quad (2.5)$$
$$W_{21} = \sigma_{21}F. \quad (2.6)$$

where σ is the cross section of the transition and has dimension of an area (barn b, where 1 b = 10^{-28} m^2 = 100 fm^2).
The cross section depends only on the characteristics of the particular transition. F is the photon flux of the EM wave and has dimension of $[\text{time}]^{-1}[\text{area}]^{-1}$.
If the two levels are non-degenerate, then $W_{12} = W_{21}$ and $\sigma_{12} = \sigma_{21}$ are valid. If the two levels are degenerate with degeneracy g_1 and g_2 respectively, then it is true that $g_1W_{12} = g_2W_{21}$ and so $g_1\sigma_{12} = g_2\sigma_{21}$ [5].

2.1.2. The idea of laser

Amplifier

Assuming two energy levels E_1 and E_2, with degeneration g_1 and g_2 and populations N_1 and N_2, respectively. An EM wave with a photon flux F propagates along the z-axis (Fig. 2.2).

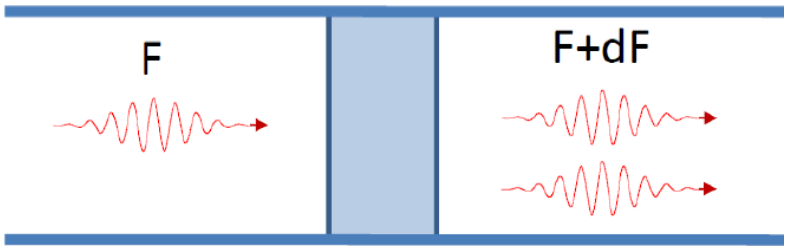

Figure 2.2. Elementary change dF in the photon flux F during the dissemination of a plane wave from the material.

The elemental change in flux dF by the elementary length dz, will be equal to the number of photons produced by stimulated emission minus those which were absorbed. So:

$$\frac{dF}{dz} = W_{21}N_2 - W_{12}N_1 = \sigma_{21}FN_2 - \sigma_{12}FN_1 = F\sigma_{21}\left[N_2 - \frac{\sigma_{12}}{\sigma_{21}}N_1\right] = F\sigma_{21}\left[N_2 - \frac{g_2}{g_1}N_1\right]. \quad (2.7)$$

The eq. 2.7 shows that the material behaves as an amplifier when $dF/dz > 0$, i.e. when $N_2 > (g_2/g_1)N_1$. Otherwise, when $N_2 < (g_2/g_1)N_1$, it behaves as an absorber.

A simple laser - cavity laser

To create a laser beam from an amplifier, a positive feedback scheme called oscillator is needed. This is achieved by placing the active medium between two highly reflective mirrors (Fig. 2.3) [6]. This structure is known as a laser cavity. As the EM wave, which goes in the direction of the two mirrors, reflects back and forth on the mirrors, it is amplified each time it passes through the active amplifier medium. By constructing one of the two mirrors partially permeable to the frequency of EM wave, the laser beam is resulted at the output of the mirror.

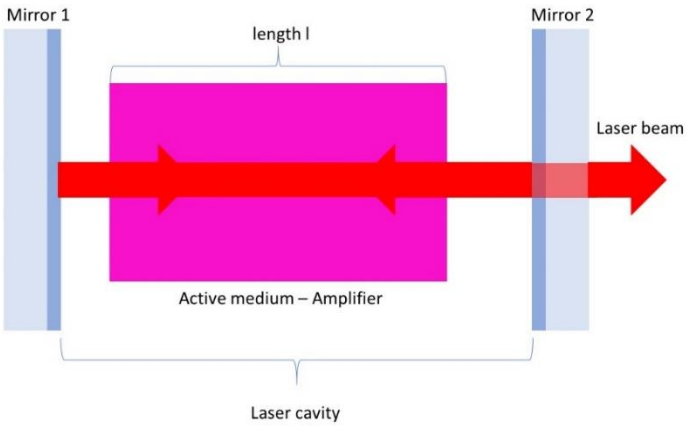

Figure 2.3. The operating principle of the laser [6].

To maintain the above procedure of the laser, it is important to achieve the so-called *threshold condition*. The threshold condition states that the gain of the active medium must compensate the losses of the cavity. From the eq. 2.7, the amplification which is achieved by a passage into the cavity is:

$$F = exp\{\sigma_{21}[N_2 - (g_2/g_1)N_1]l\}, \tag{2.8}$$

where l is the length of the active medium. R_1 and R_2 are the reflectivity of the two mirrors and L_i is the internal loss for each pass in the cavity. Whether at a given moment, the photonic flux in the cavity which leaves from the mirror 1 towards the mirror 2 is F, then for the flow F' at the same point after a circle in the cavity is:

$$F' = Fexp\{\sigma_{21}[N_2 - (g_2/g_1)N_1]l\} \times (1 - L_i)R_2 \times exp\{\sigma_{21}[N_2 - (g_2/g_1)N_1]l\} \times (1 - L_i)R_1,$$

$$F' = Fexp\{2\sigma_{21}[N_2 - (g_2/g_1)N_1]l\} \times (1 - L_i)^2 R_1 R_2 \,. \tag{2.9}$$

In threshold conditions F = F '. So

$$exp\{2\sigma_{21}[N_2 - (g_2/g_1)N_1]l\} \times (1 - L_i)^2 R_1 R_2 = 1. \tag{2.10}$$

From the above equation, the threshold conditions are reached when the population inversion acquires the following critical value is called the critical inversion:

$$N_c \equiv N_2 - (g_2/g_1)N_1 = -\frac{\ln(R_1 R_2) + 2\ln(1 - L_i)}{2\sigma_{21} l}. \tag{2.11}$$

The eq. 2.9 is simplified by introducing the variables

$$\gamma_1 \equiv -\ln(R_1) = \ln(1 - T_1). \tag{2.12.a}$$
$$\gamma_2 \equiv -\ln(R_2) = \ln(1 - T_2). \tag{2.12.b}$$
$$\gamma_i \equiv \ln(1 - L_i). \tag{2.12.c}$$

wherein T_1 and T_2 are the transmissions of the mirrors 1 and 2, respectively.

Then, the eq. 2.11 is formed as below:

$$N_c \equiv {}^{\gamma}/_{\sigma l}\,, \tag{2.13}$$

where $\sigma \equiv \sigma_{21}$ and

$$\gamma = \gamma_i + \frac{\gamma_1+\gamma_2}{2}. \tag{2.14}$$

The γ_i is called the logarithmic internal loss of the cavity. It is usually $L_i \ll 1$, so $\gamma_i \cong L_i$. The γ is called the single-pass loss of cavity [5].

The oscillation of the laser proceeds through the spontaneous emission when the threshold condition is reached. The spontaneous emission photons actually begin their amplification process, i.e. the laser [4].

2.1.3. Pumping

This section deals with how it can be achieved a population inversion in the material which acts as an amplifier. In a two-level system, a population inversion is not possible. Thus, systems with more levels should be used. The most common systems are those of three-level laser, like a Ruby laser [22] and four-level laser, like Ti:sapphire laser [20] and an Nd:YAG [21].

Three – level laser: The atoms are excited from the ground state (level 1) at excited state (level 2). Then, the atoms are rapidly decayed to level 3 (possibly through a non-radiative decay). If the decay from level 3 to the ground state is much slower than the decay from level 2 to level 3, then the conditions of a population inversion are achieved.

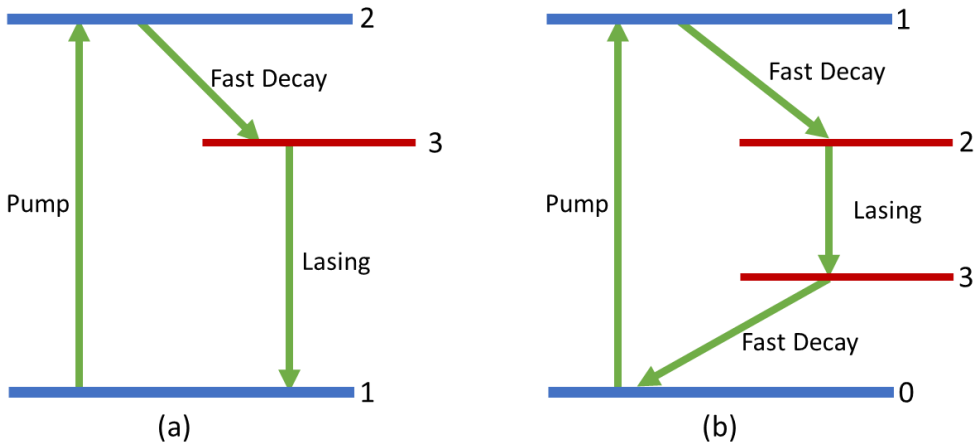

Figure 2.4. (a) a three-level laser, (b) a four-level laser [4].

Four – level laser: The atoms are excited from ground state (level 0) to excited state (level 1). Then, the atoms are rapidly decayed to level 2 (possibly through a non-radiative decay). If the decay from level 2 to level 3 is much slower than the decay from level 1 to level 2, then the conditions of a population inversion are achieved.

It is important to note that the system has to return to the ground state and close the cycle, so the transition from level 3 to level 0 must also be very fast (possibly again through a non-radiative decay).

The process of excitation from the ground state to the upper excited state is called *pumping*. It is easier to achieve conditions of a population inversion in a four-level laser than a three one. To achieve conditions of a population inversion in the three-level laser, it is necessary, from equation 2.7, $N_2 > N_1$ to be valid. Therefore, the population of level 2 (level 3 in Fig. 2.4.a) should be first equal to the population of the level 1 in order to start the laser process. On the other hand, in the four-level laser, due to the fact that the level 1 (level 3 in Fig. 2.4.b) is empty, the population inversion and therefore the laser process, starts from the first excited level to level 2 [6].

2.2. Wavelength selection

The gain bandwidth of the Ti:sapphire laser is broad and due to the cavity resonates at many modes, it is observed a wide output linewidth. For the wavelength selection for the Ti:sapphire laser it is used some optical elements like etalons and birefringent filters, in order to limit the broad of the output linewidth. Etalon consists of two parallel partially reflecting surfaces while birefringent filter is used to restrict the laser linewidth and the method to achieve this, is to modify the polarization of the incident beam [5].

2.3. Diffraction grating

The diffraction grating consists of many parallel and spaced slits with the distance d between the successive slots (groove spacing d). The grating is made by cutting parallel and spaced grooves on glass or metal plate where there are reflection and transmission grating [2].

For constructive interference, there is the following equation:

$$d \sin\theta = m\lambda, \tag{2.15}$$

where m is the diffraction order and is an integer, θ is the diffraction angle and λ is the wavelength of the light.

For two successive grooves, the optical path difference between them is $d * \sin a + d * \sin\theta$, where α is the angle of incidence. Thus, the eq. 2.15 for the two successive grooves becomes:

$$d * (\sin a + \sin\theta) = m\lambda. \text{ (Grating equation)} \tag{2.16}$$

When the light is diffracted back in the same direction from which it came, the angle of incidence is equal to the diffraction angle $(\alpha = \theta)$. This is called the *Littrow configuration* [7].

Thus, the grating equation is simplified to:

$$2d \sin\alpha = m\lambda. \tag{2.17}$$

It is known that the resolving power R of a grating is $R = \frac{\lambda}{\Delta\lambda}$. However, the R is also given by $R = mN$, where N is the number of illuminated grooves, $d = \frac{1}{N}$.

So, $\frac{\lambda}{\Delta\lambda} = mN$.

More details of the grating diffraction could be found in [8].

2.4. Ti:sapphire medium

In this laser, trivalent (3-valent) titanium ions (Ti^{3+}) replace some Al^{3+} ion in the crystal lattice of the Al_2O_3. The trivalent titanium ions are located on the center of an octahedral crystal structure. The trivalent ion of titanium, which is a transition element, has only one 3d electron in the outer electron shell, which has strong coupling to the lattice of the receiving material. The effect of the strong coupling of the 3d electron to the lattice is the significant widening of the energy levels, creating a wide absorption range [9].

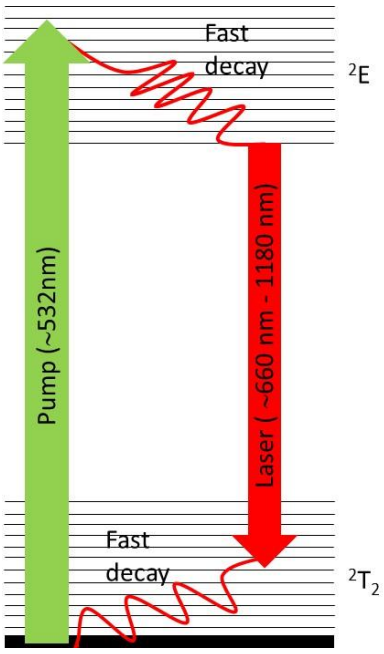

Figure 2.5. Ti:sapphire structure of energy levels [2].

In Fig. 2.5, it is observed that the pump laser excites the electron from the lowest vibrational level of $^2T_2$ state to the vibrational states of ^2E. Then, the electron rapidly relaxes into the basic state of ^2E. Their lifetime is of the order of μs, therefore it is suitable for inversion of the population. The decay from the basic state of ^2E to some of the excited vibrational states of $^2T_2$ provides the laser. Then, an additional quickly decay occurs in the basic vibrational state of $^2T_2$. Thus, the Ti:sapphire laser is a four-level laser [6].

The Ti:sapphire lasers can be pulsed or be continuous (CW). In the CW mode, they emit a few Watts when pumped to the maximum absorption of their ground states, i.e. ~ 500 nm. The Ti:sapphire laser is a variable wavelength laser and its emission band is from 660 to 1180 nm [4].

2.5. Atom – light interaction (Saturation)

During the resonance ionization spectroscopy, it is important to examine the interaction of the light fields with the multi-atomic levels. For convenience, it is used a simple two-level system with the ground state and the excited state. The population density of the excited state is given as:

$$p = \frac{1}{2}\frac{S}{1+S}, \tag{2.18}$$

where $S = \frac{S_o}{1+(\frac{2\delta}{\gamma})^2}$.

Thus,

$$p = \frac{1}{2}\frac{S_o}{(S_o+1)}\frac{1}{1+\frac{4\delta^2}{\gamma'^2}}. \tag{2.19}$$

The factor γ is the decay constant of the excited state (the inverse of the lifetime of the state) and $\delta = \omega_L - \omega_{eg}$, detuning of the laser frequency ω_L.

It is known that $S_o = \frac{I}{I_{sat}}$ is the resonant saturation parameter and I_{sat} is the saturation intensity, $I_{sat} = \frac{\pi hc}{3\lambda^3\tau}$. The factor λ is the laser wavelength and τ is the excited state lifetime.

When $S_0 \ll 1$, the population is mainly in the ground state. In the case $S \gg 1$, the population is equally distributed between the ground and the excited state [10].

It is important to note that the profile of the population density p is a Lorentzian function with FWHM of

$$\gamma' = \gamma\sqrt{1+S_o}\,. \tag{2.20}$$

The eq. 2.20 depends on the intensity of the laser. This phenomenon is called saturation broadening [2].

2.6. Resonance Ionization Spectroscopy

The resonance laser ionization is a mechanism through an atom is excited and a valence electron is promoted to a higher atomic level. If the transitions take the valence electron over the ionization potential (IP) of the atom, the ionization is possible to be happened.

The excitation energy of the atomic states of each element is the fingerprint of the atomic states. Thus, the mechanism of the resonance laser ionization could be used in order to give the element specific ionization.

The process of the ionization could be used to optical spectroscopy in the form of Resonant Ionization Spectroscopy (RIS). RIS was developed in the early 1970 [11].

The most common mechanisms of ionization are the following. At first, there is the ionization through an auto-ionizating (AI) state. During auto-ionization, the ionization potential is energetically lower than the transition, which is usually called as AI state. The AI formations are come from multi-electron excitation in the atom. In AI states, high cross sections are observed for excitation, which leads to rapid ionization ($\sigma_I \sim 10^{-15} cm^{-2}$).

Then, there is the Rydberg ionization. This type of ionization happens at an energetically state, just below the IP. The ionization could be caused by IR radiation, electrostatic fields or collisions with the other atoms. The last one is the non-resonant ionization. It happens with non-resonant laser radiation, and after the first or the second resonant transition. The disadvantage of this type of ionization is that the ionization cross section is lower in comparison with the cross section for resonant excitation. The cross section is around $\sigma_I \sim 10^{-17} cm^{-2}$[12].

The Fig. 2.6 shows these three mechanisms.

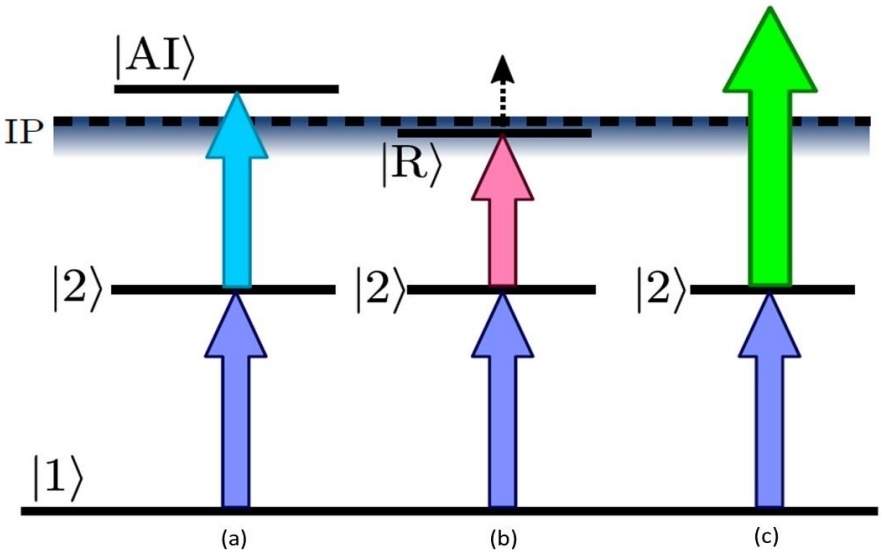

Figure 2.6. Ionization mechanisms. (a) Auto-ionization, (b) Rydberg ionization and (c) non-resonant ionization [13].

3. Experimental setup and tools

This chapter deals with the description of the experimental setup which is used, its parts, as well as, the setup and layout of electronics.

3.1. Experimental setup

The optical tables 1 and 2 depict the schematic layout of the laser setup which is used. For the first part of the thesis is used the self-seeded grating-based Ti:sapphire laser from the optical table 2, while for the second part both optical tables are used.

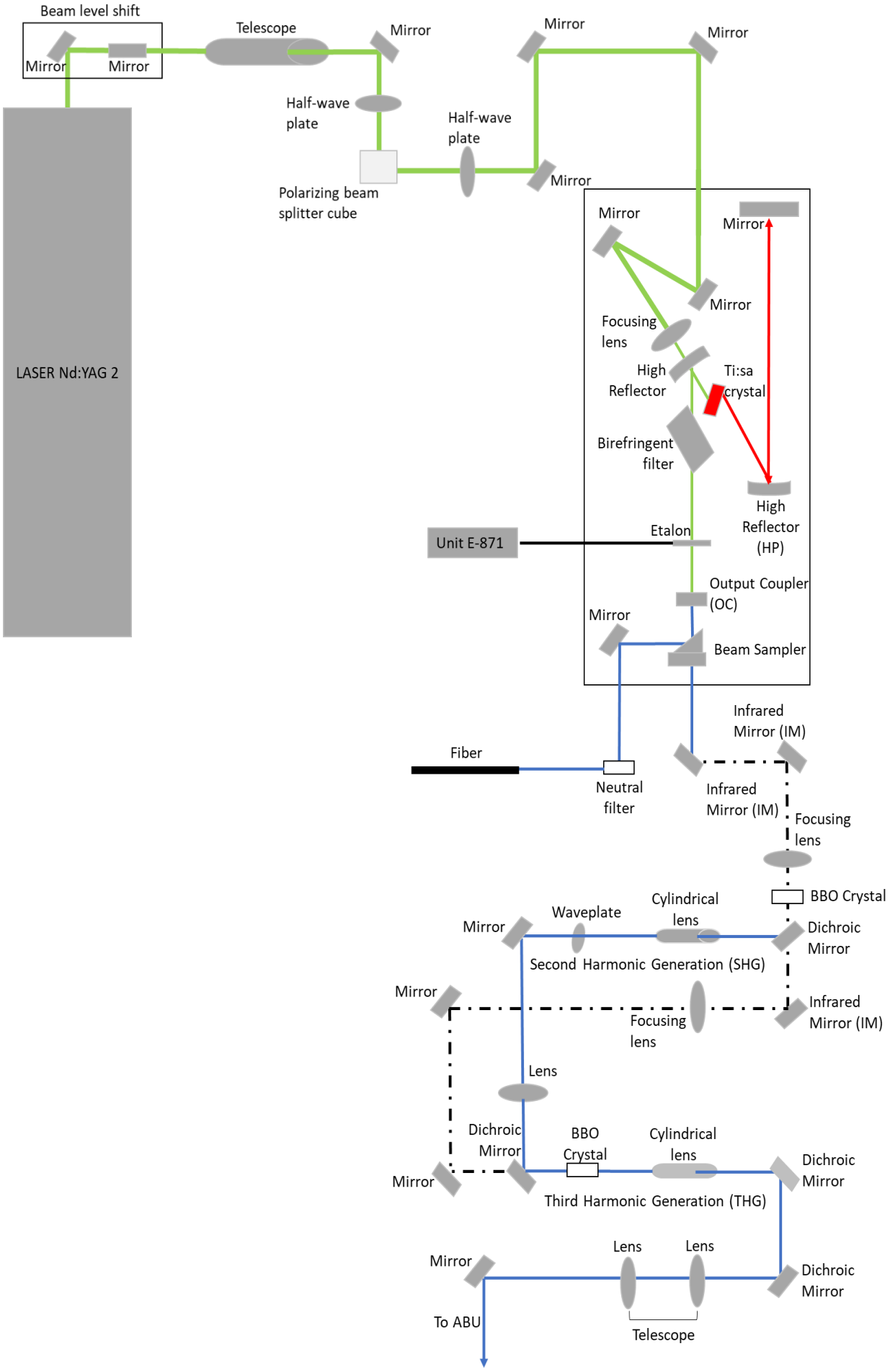

Figure 3.1. Schematic layout of the laser setup for optical table 1.

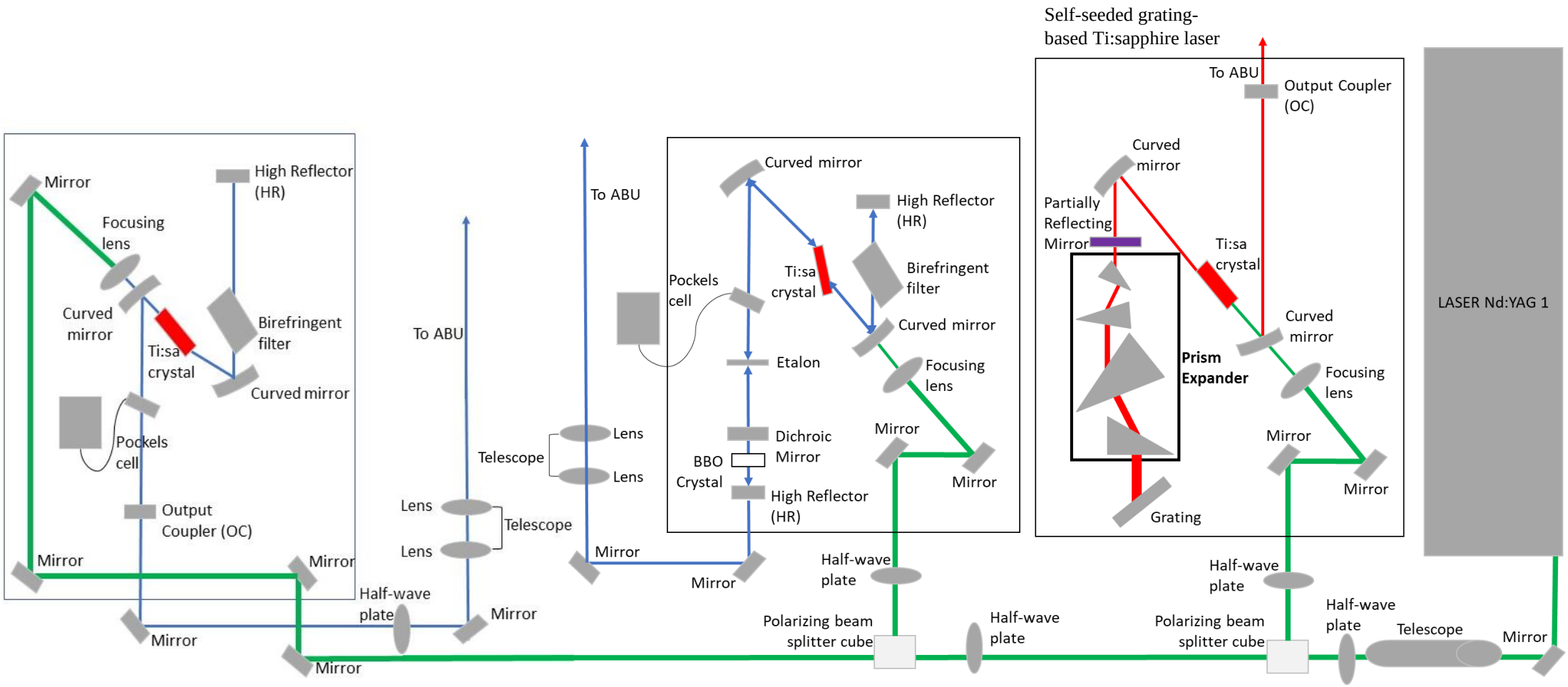

Figure 3.2. Schematic layout of the laser setup for optical table 2.

The pump laser Nd:YAG 2 (Lee Laser, LDP-200MQG, QEM model, second hand) is set at 24W output power of the second harmonic at 532 nm with 10 kHz of pulse repetition rate while Nd:YAG 1 (Lee Laser, LDP-200MQG) is set at 14.9W output power of the second harmonic at 532 nm with 10 kHz of pulse repetition rate [2]. Telescope, which consists of two lens and increases the beam spot (beam expander), half-wave plates, mirrors and polarizing beam splitter cubes are used in order to divide the output power from the pump laser Nd:YAG 1. Then, the output power is allocated to the Ti:sapphire systems. The wave plate is used to control the polarization state of light. The half-wave plate is a type of wave plate and shifts the polarization direction of linear polarized light.

The cavity design of the Ti:sapphire laser was developed at the University of Mainz and the shape is Z-shape. It consists of two curved mirrors (CM), a flat high reflector (HR), an output coupler (OC), an etalon (frequency selection), a PC (timing) and a birefringent filter or a Lyot – Filter (frequency selection). The one surface of the CMs is coated with high reflection for the laser wavelength, while the other surface is coated in order to limit the wavelength of the pump laser. A focusing lens, which is before the first CM, is used in order to focus the pump laser on the Ti:sapphire crystal, which is located between the two CMs [14].

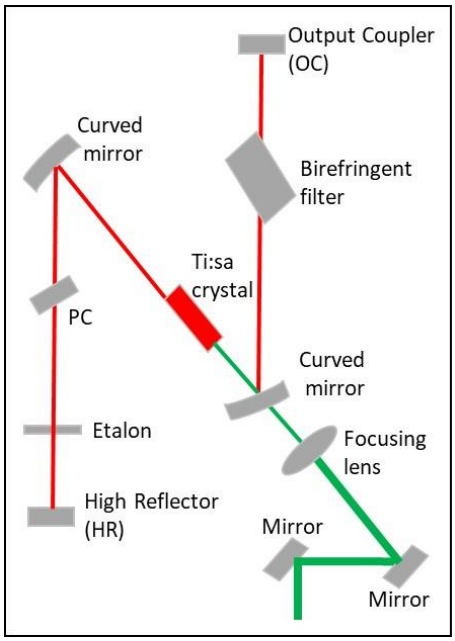

Figure 3.3. Schematic layout of a standard pulsed Ti:sapphire cavity.

Other parts of the setup are birefringent filters which are used to restrict the laser linewidth and the method to achieve this, is to modify the polarization of the incident beam [6]. At the same time a birefringent crystal, BBO (βeta-Barium-Borate) extends the range of the Ti:sapphire to higher harmonic generation. At the optical table 1, the output coupler (OC), flat reflective mirror, extracts the laser beam with a reflectivity of 90%. At the optical table 2, in the self – seeded grating – based Ti:sapphire cavity, the OC has 80% reflectivity and the last OC has 70% reflectivity. As a harmonic separator operates the dichroic mirror. It is a mirror which has different reflection or transmission properties at two different wavelengths [15].

Also, some other components that are used in optical table 1 and 2 are prism expander, etalon, polarizing beam splitter cube, focusing lens, high reflector (HR), beam sampler, infrared mirror, cylindrical lens, curved mirror, partially Reflecting (PR) mirror and the grating. Pockets cells are electro-optical crystals and operate as a voltage-controlled wave plate and are used in order to synchronize the Ti:sapphire lasers. If an appropriate voltage is applied to the crystal, then the polarization of the passing light is rotated by 45^o and is reflected from the reflective mirror and passes again from the crystal which is under voltage. Thus, the polarization is rotated again by 45^o. The total rotation is 90^o relative to the original polarization. For more details, address to Ref [9, 15, 16]

The last part of the setup is the Atomic Beam Unit or ABU. ABU is a useful tool for off-line laser spectroscopy. It is used for laser excitation tests and developments of ionization schemes. It consists of a thin tantalum tube, which is heated electrothermally in order to reach a sufficient temperature, up to 1600^oC, and the sample of material to evaporate [12]. Then, the atomic beam passes through a small hole (orifice) and is collimated. Behind the small hole is located an electrode with a positive potential of +80 V. This electrode is used in order to have better background signal of the thermal ions derived from the tantalum tube [2]. The collimated beam and the laser interact with each other in the interaction region. The ions of the laser are directed to electron multiplier tube (EMT) and a potential of -2.5kV is applied.

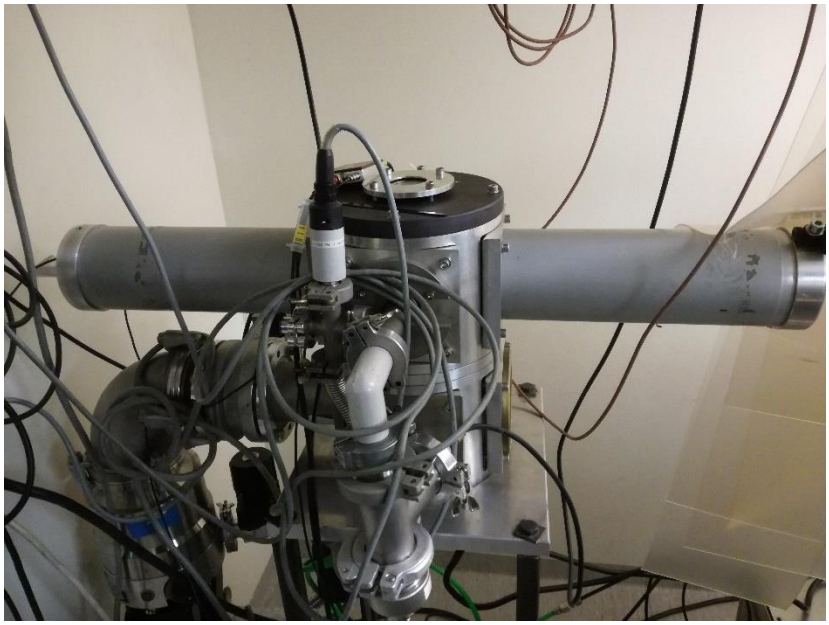

Figure 3.4. ABU unit.

3.2 Electronic setup

To extract the important information, an appropriate electronic setup is necessary.

For the laser timing, there is external frequency generator – Agilent 33120A (master clock) provides the 10kHz external trigger (signal TTL). The signal allocates to two GDG units (model 416A, Nd:YAG 1 timing and Nd:YAG 2 timing). The individual signals are then sent to the two pump lasers Nd:YAG 1 and Nd:YAG 2. The pump lasers can be synchronized over time with the suitable settings of the GDGs.

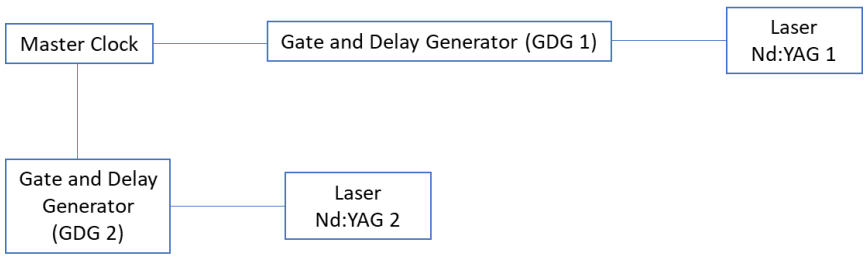

Figure 3.5. Laser time setup.

For the data acquisition, the first stage in the electronic chain is the preamplifier (ORTEC – VT120 Fast Timing Preamplifier), which is connected to the ABU. The role of the preamplifier is to extract the signal from the detector with as little amount of noise as possible. This is why the preamplifier is located as close as possible to the detector [17]. The preamplifier is then connected to the amplifier (ORTEC – FTA820A Octal Fast Timing Amplifier). The signal, now, is amplified and takes the appropriate shape for more extensive processing. Next, the amplifier is connected to the discriminator (ORTEC – 584 Constant Fraction Discriminator), which eliminates background noise and is used as an analog to digital converter [17]. The CF Disc is linked with the Coincidence unit (takes only the negative signal). Here, an oscilloscope (Rigol DS1204B 200MHz Digital Oscilloscope) checks the positive signal. Also, it is used a master clock (external frequency generator – Agilent 33120A), which is connected with the Gate and Delay Generator (GDG – model 416A). The GDG is connected with the Coincidence unit. Finally, the signal from the Coincidence unit goes to a second GDG (model 416A) unit to make the signal suitable for the Counter, which is connected to the computer.

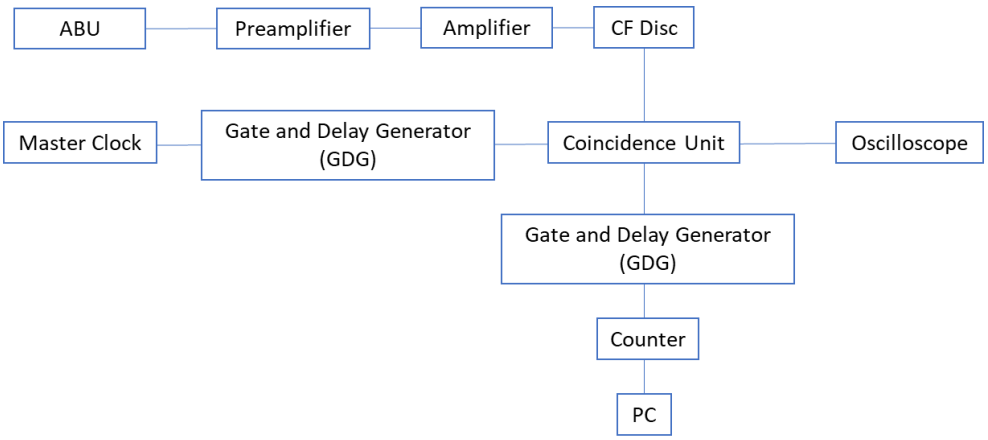

Figure 3.6. Data acquisition setup

4. A self-seeded grating-based Ti:sapphire

4.1. Experimental Setup

The setup of the self-seeded grating-based Ti:sapphire laser is similar to the standard Ti:sapphire laser, i.e. it has a Z-shaped design. However, there are some differences.

The self-seeded grating-based Ti:sapphire laser consists of two curved folding mirror (CM) with the range of reflective coating to fluctuate between 650nm - 1050nm. The output coupler (OC) with 80% reflectivity has a similar range of reflective coating with the CMs. In addition, there is a focusing lens, which is located before the first CM, and it is used to focus the pump laser on the Ti:sapphire crystal. The Ti:sapphire crystal is pumped by the 532nm second harmonic of a Nd:YAG laser operating at 10kHz repetition rate. After the second CM, there is a partially reflecting (PR) mirror and then a prism beam expander. Instead of a high reflector mirror (HR) which exists in the standard Ti:sapphire, the cavity is closed with a diffraction grating in Littrow configuration. The grating is a gold coated diffraction grating with 1500 grooves/mm. Therefore, one more cavity is formed consisting of the PR mirror, the prism beam expander and the grating. The prism beam expander is inserted into the cavity because the grating is sensitive to high power densities. That can be overcome by expanding the laser beam diameter.

The schematic layout of the self-seeded grating-based Ti:sapphire laser and pictures from the laboratory about the Ti:sapphire cavity are shown in Fig. 4.1 and Fig. 4.2.

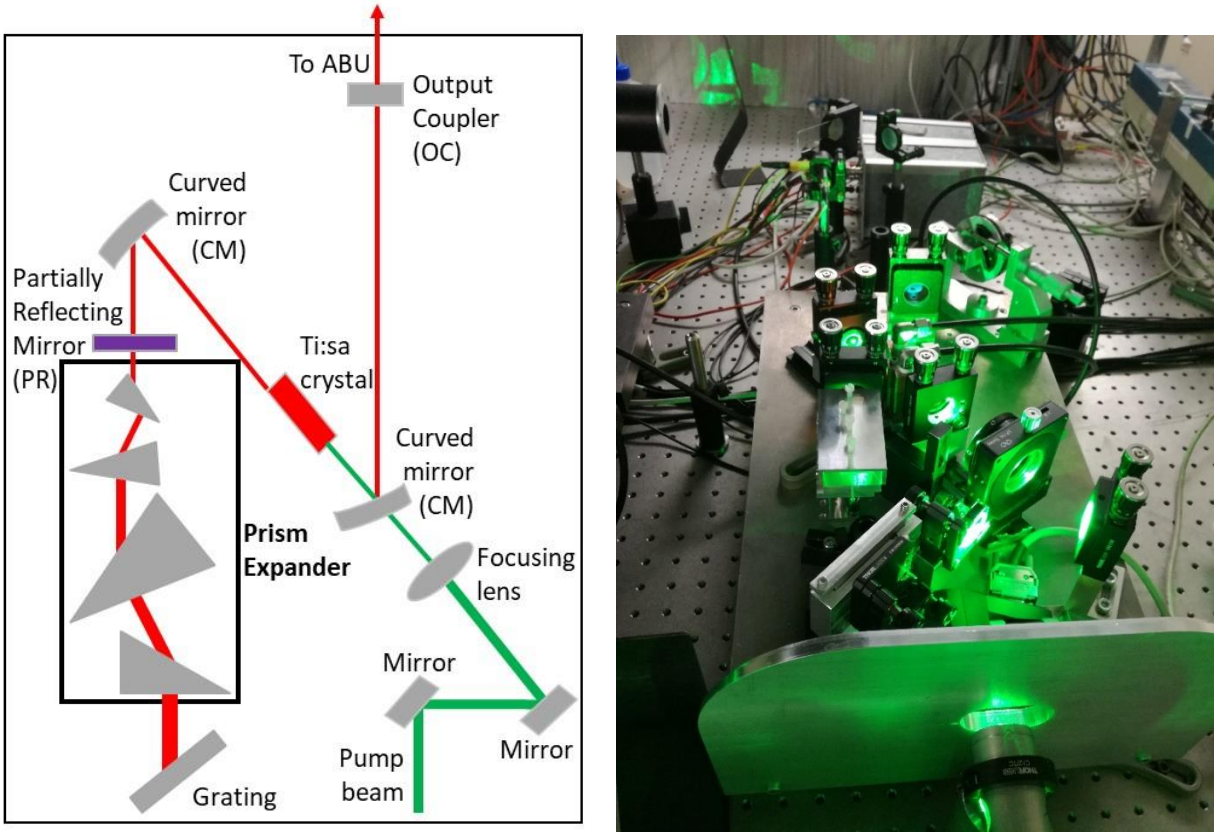

Figure 4.1. Picture 1 and schematic layout of the self-seeded grating-based Ti:sapphire laser.

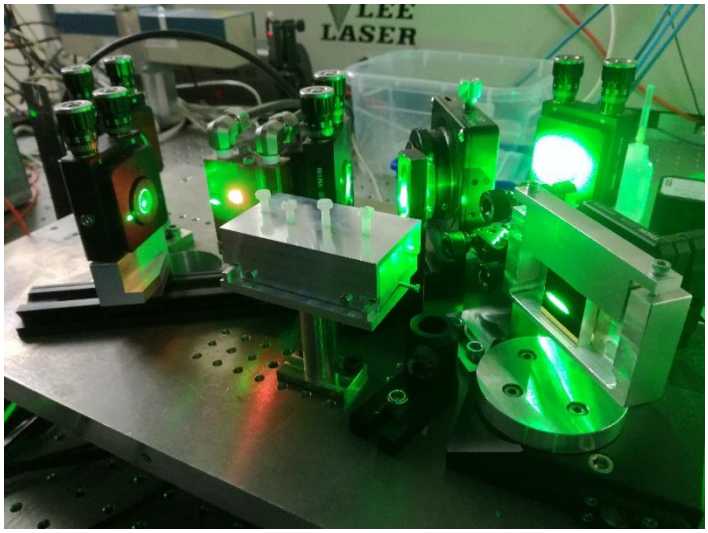

Figure 4.2. Picture 2 of the classic grating-based Ti:sapphire.

4.2. Experimental results

4.2.1. Output power

To increase the fundamental output power, it is necessary to use the partially reflecting mirror. The goal is to achieve the highest output power improvement compared to the non-seeded resonator, i.e. the classic grating laser. The classic grating laser is without the PR mirror.

Set the pump power to 14.9A. First, the cavity of the classic grating laser is used. The Fig. 4.3 shows the output power as a function of the wavelength.

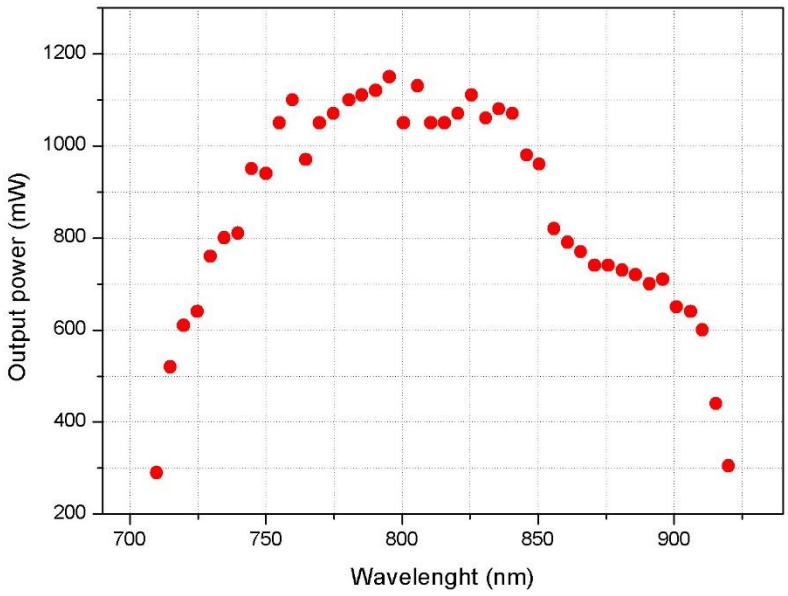

Figure 4.3. Output power as a function of wavelength for the classic grating laser.

Four PR mirrors with different reflectivities are then tested. The PR mirror is inserted in the cavity between the second CM and the prism beam expander.

The first PR mirror being tested has 30% reflectivity. The Fig. 4.4 shows the PR mirror and some of its characteristics. The output power as a function of the wavelength for the extended self-seeding cavity is depicted in Fig. 4.5

Figure 4.4. Partially reflecting mirror with 30% reflectivity.

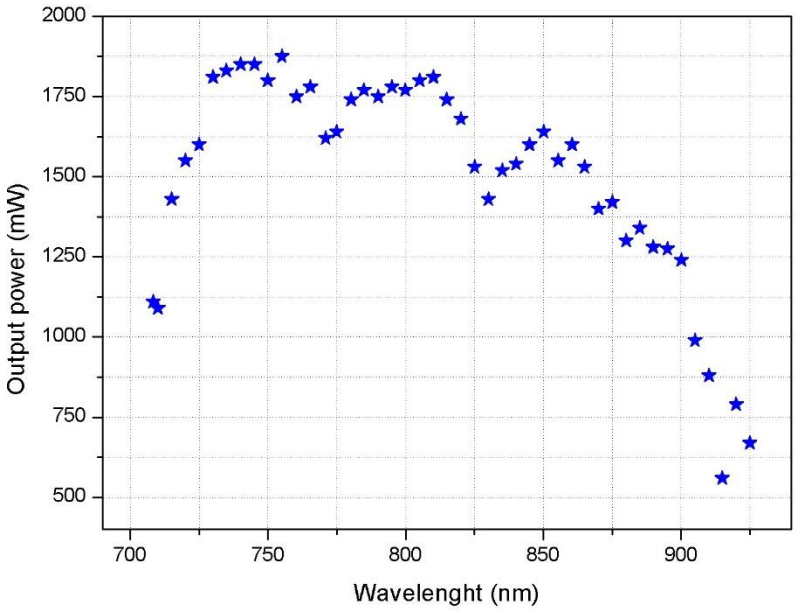

Figure 4.5. Output power as a function of wavelength for the self-seeded grating-based Ti:sapphire laser using mirror with 30% reflectivity.

Then, the PR mirror with 30% reflectivity is replaced by a PR mirror with 48% reflectivity. Similarly, the Fig. 4.6 shows the PR mirror and some of its characteristics and the Fig. 4.7 describes the output power as a function of the wavelength for this case.

Figure 4.6. Partially reflecting mirror with reflectivity of 48%.

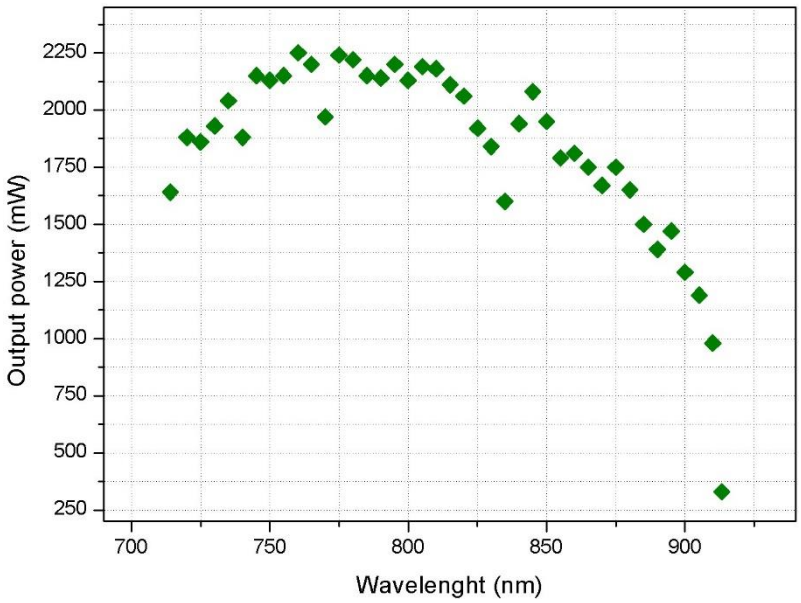

Figure 4.7. Output power as a function of wavelength for the self-seeded grating-based Ti:sapphire laser using mirror with 48% reflectivity.

Next, the PR mirror with 70% reflectivity is used. Using this PR mirror and the pump power at 14.9V, some difficulties arise. It does not show additional seeding effects as a result (such as bad mode from reflectivity and) low output power. Hence, the pump power is increased to 15.4V in order to eliminate the difficulties. The result is shown in Fig. 4.8.

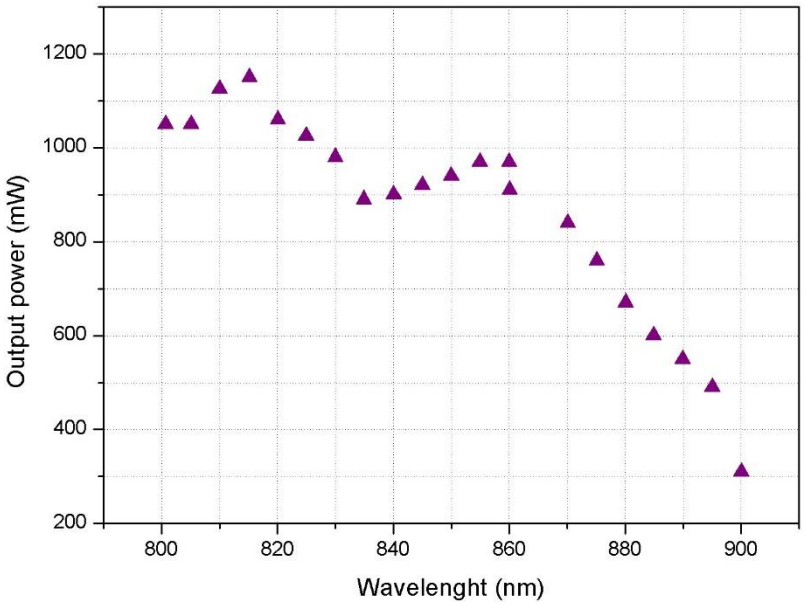

Figure 4.8. Output power as a function of wavelength for the self-seeded grating-based Ti:sapphire laser using a mirror with 70% reflectivity.

Figure 4.9. Partially reflecting mirror with 70% reflectivity.

For the PR mirror with a reflectivity of 80%, the same difficulties arise. However, here it is not possible to eliminate the difficulties by increasing the pump power. The Fig. 4.10 shows the PR mirror and some of its characteristics.

Figure 4.10. Partially reflecting mirror with reflectivity of 80%.

The mirrors with 70% and 80% reflectivity are not used further, due to no additional seeding effects.

To see the effect of the PR mirror in order to achieve the highest output power improvement compared to the non-seeded resonator the Fig. 4.11 is created.

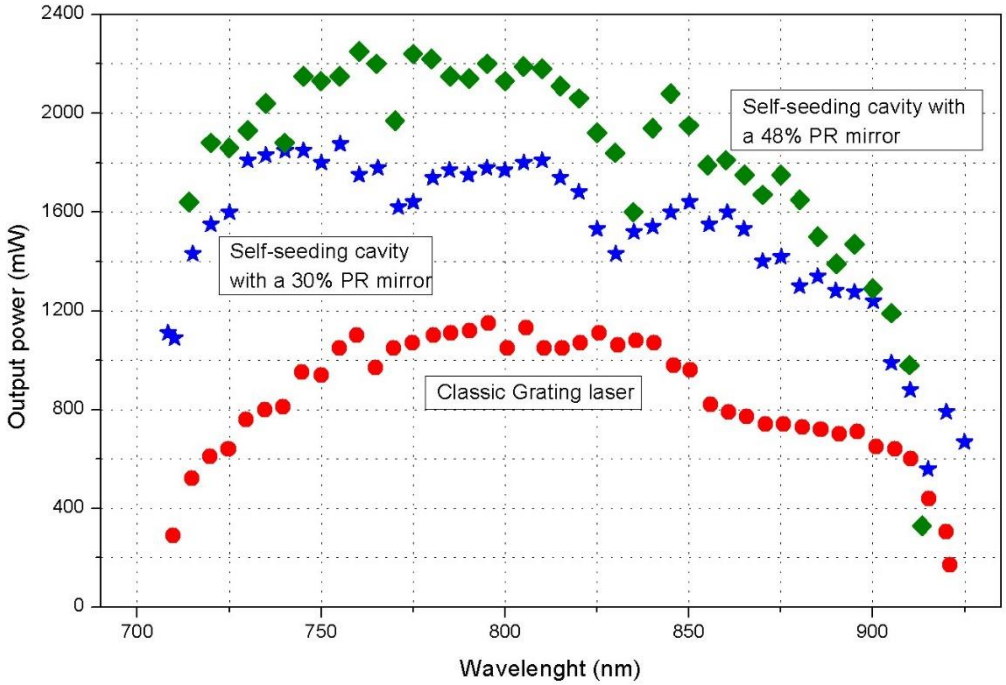

Figure 4.11. Output power as a function of wavelength for the classic grating laser compared with the extended self-seeding cavity using a PR mirror with 30% and 48% reflectivity.

The highest output power is achieved in the cavity with the 48% PR mirror and the fundamental output power is bigger than the classic cavity grating laser by a factor of 2.

4.2.2. Ratio of power

For extended self-seeding cavity with the 48% PR mirror, the ratio of power is calculated. The ratio of power is calculated from the non-seeding power to the output power. Thus, the Fig. 4.12 depicts the ratio of power as a function of the wavelength.

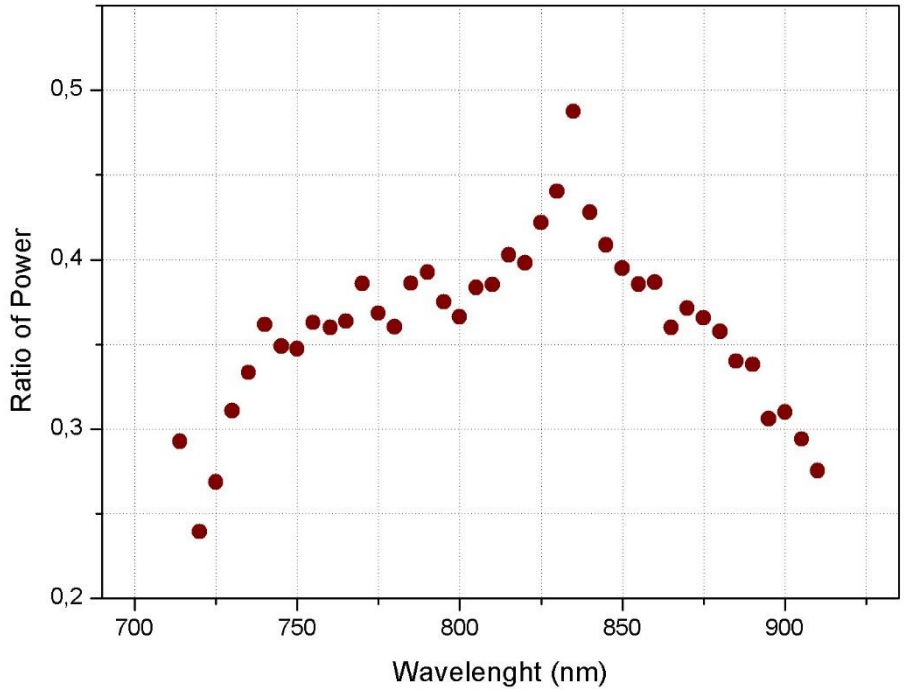

Figure 4.12. Ratio of power Vs wavelength for the self-seeded grating-based Ti:sapphire laser cavity with 48% PR mirror.

4.2.3. Temporal profile

The motivation of this part of the thesis arise from the desire to insert a frequency – doubling crystal between the Output Coupler (OC) and the first Curved mirror (CM).

The distance between the OC and the zero point changes in the self-seeding cavities with 30% and 48% reflecting mirrors. The zero point is located as close as possible to the first CM but without affecting the Ti:sapphire crystal. By changing the distance and having a constant wavelength, the following diagrams are created in order to find the pulse width for various distances. Using Gaussian distribution, the pulse width is the FWHM. For the measurements is used fast photodiode due to the short pulse duration. The fast photodiode is connected with the oscilloscope in order to see the pulse. The oscilloscope gives point from 0 to 10000. The time between these points is 1000ns. So, in order to calibrate the x axis and calculate the pulse width, it is necessary to divide the time with the index of oscilloscope. Thus, the correct calibrated x axis is with 0.2 ns.

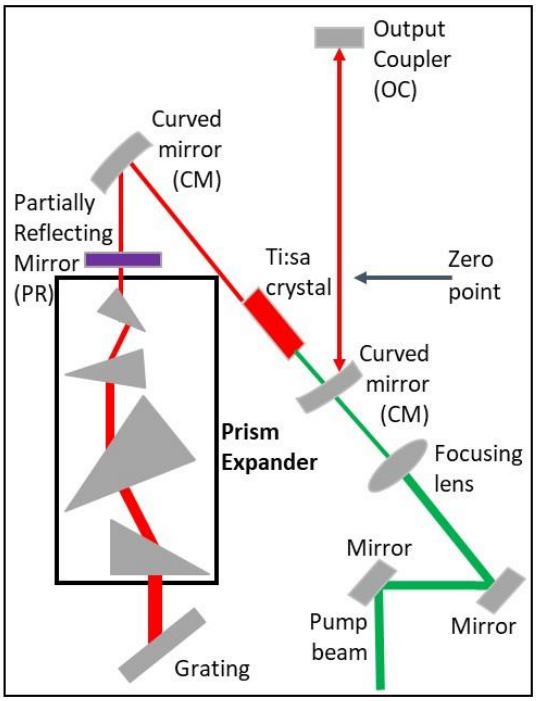

Figure 4.13. Schematic layout of the self-seeded grating-based Ti:sapphire laser, in which the change in the distance between the OC and the zero point is observed.

For the self-seeding cavities with 30% PR mirror.

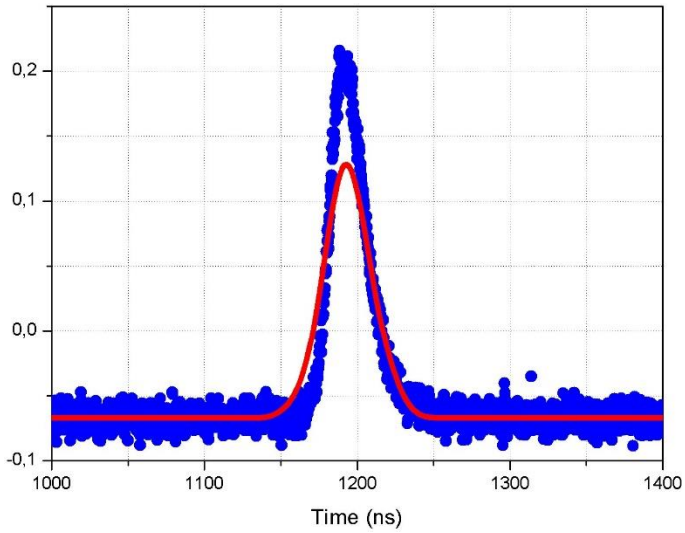

Figure 4.14. Pulse with $FWHM = 27.00294\ ns$ when the distance is 0.5 cm.

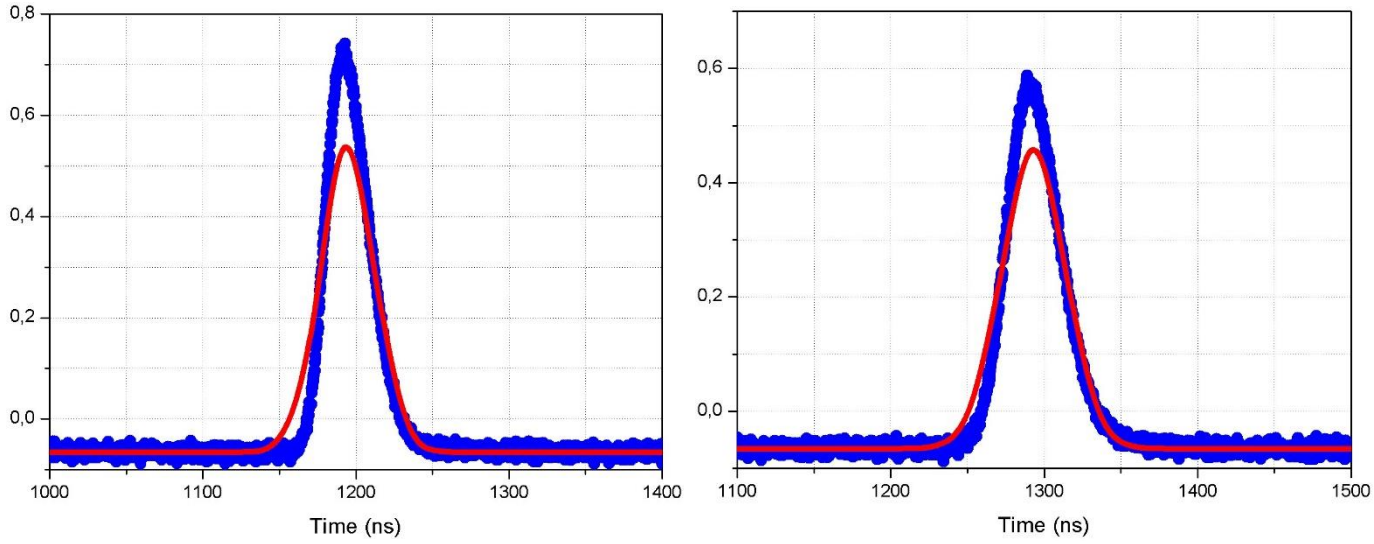

Figure 4.15. Left: Pulse with $FWHM = 32.25363\ ns$ when the distance is 1.7 cm. Right: Pulse with $FWHM = 40.84338\ ns$ when the distance is 5 cm.

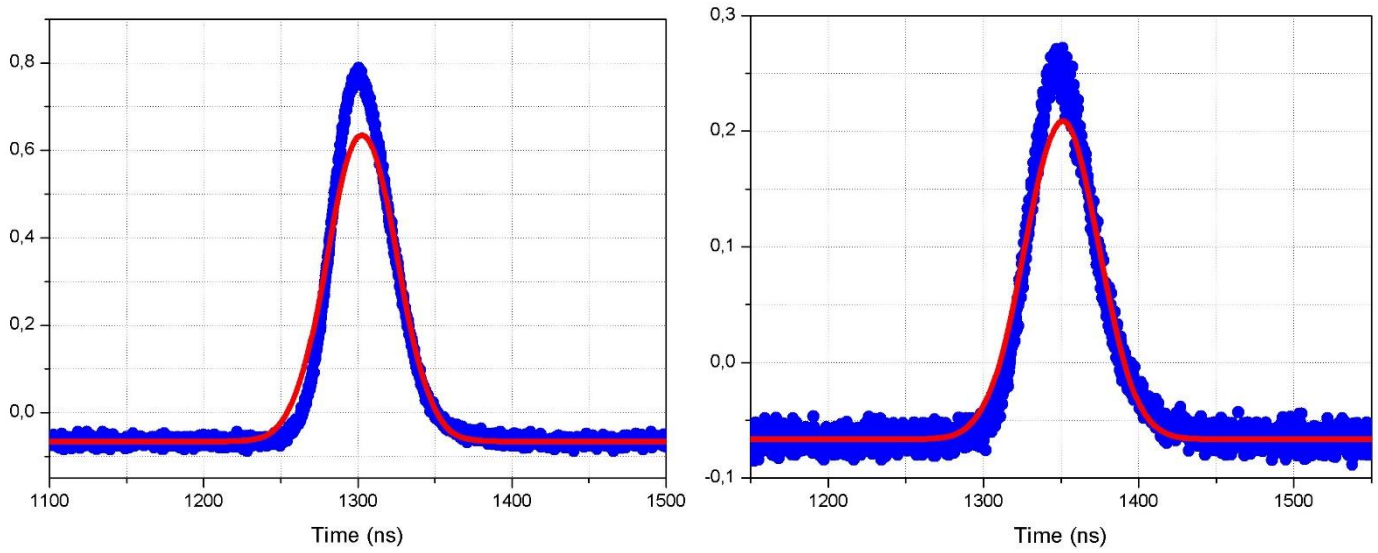

Figure 4.16. Left: Pulse with $FWHM = 44.52934\ ns$ when the distance is 6.1 cm. Right: Pulse with $FWHM = 48.81766\ ns$ when the distance is 9.1 cm.

For the self-seeding cavities with 48% PR mirror.

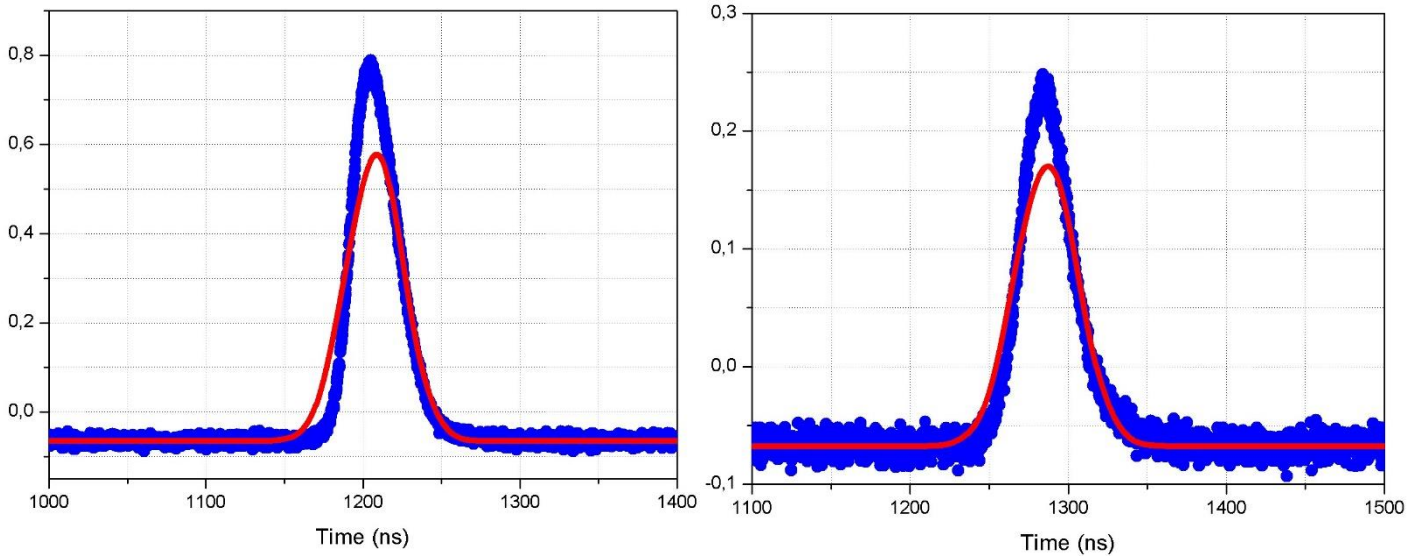

Figure 4.17. Left: Pulse with $FWHM = 33.27056\ ns$ when the distance is 0.1 cm. Right: Pulse with $FWHM = 38.1328\ ns$ when the distance is 5.8 cm.

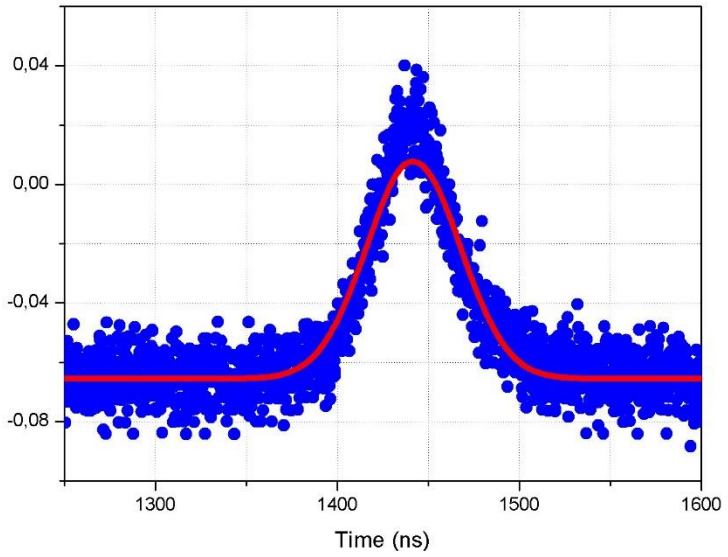

Figure 4.18. Pulse with $FWHM = 53.91285\ ns$ when the distance is 8.2 cm.

By having the pulse width for various distances, it is important to check the relation between distance with the pulse width and the output power.

For the self-seeding cavity with 30% PR mirror, the left panel of Fig. 4.19 shows the pulse width as a function of distance while the output power as a function of distance is depicted in the right panel.

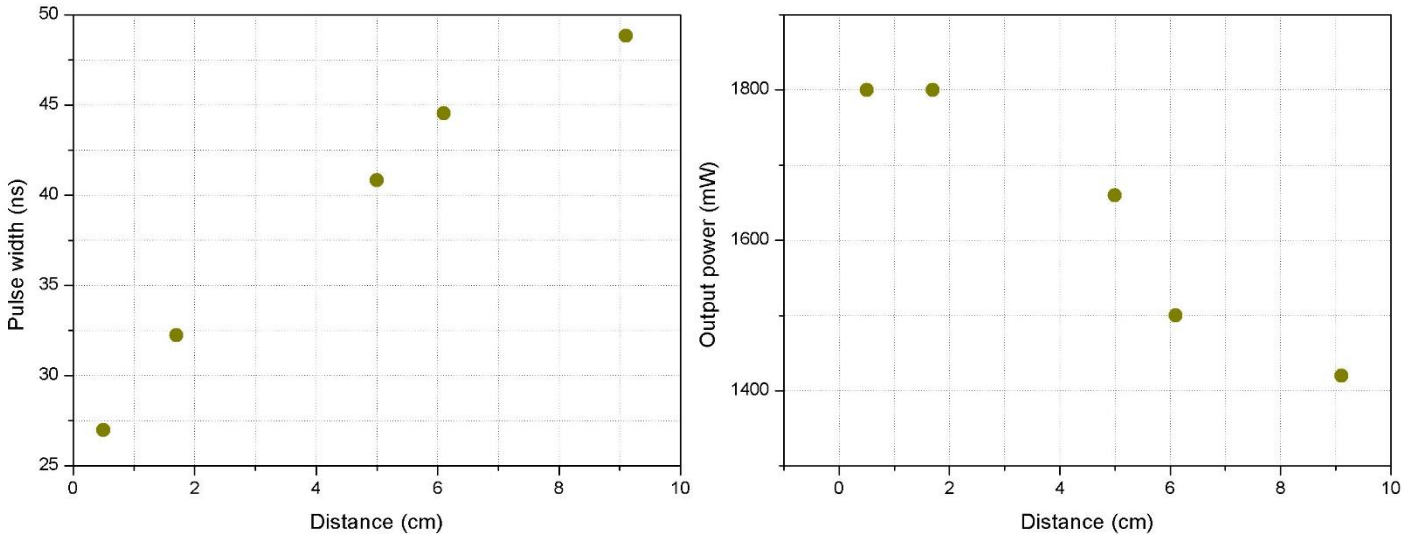

Figure 4.19. Left: Pulse width as a function of distance. Right: Output power as a function of distance.

Similar for the self-seeding cavity with 48% reflecting mirror.

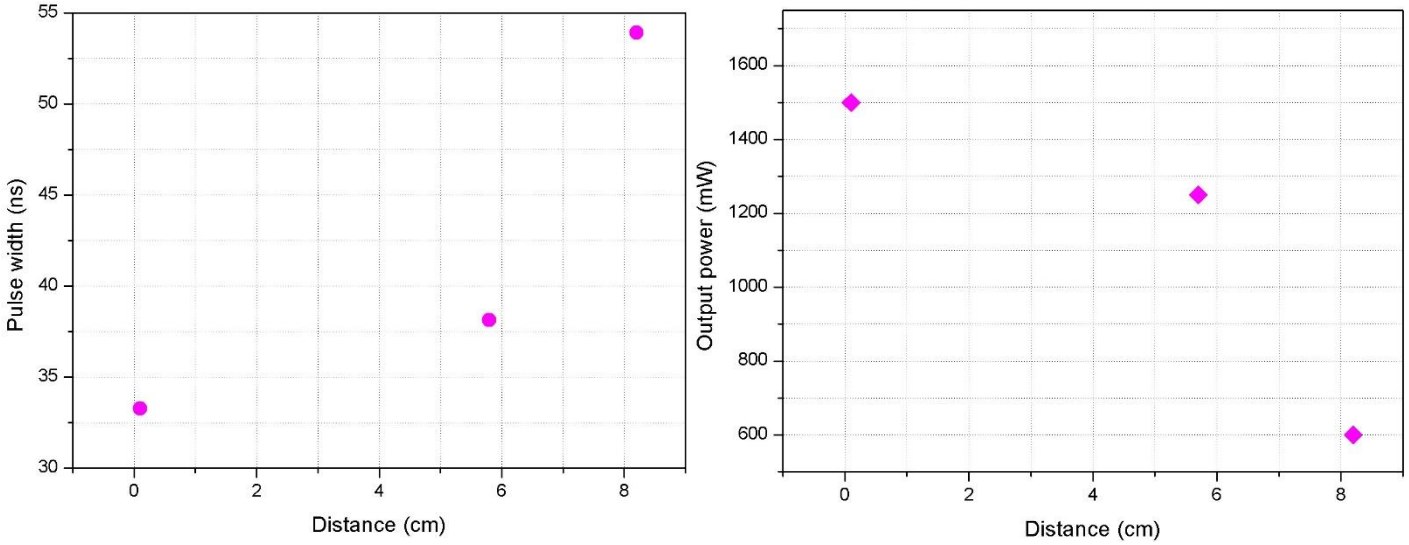

Figure 4.20. Left: Pulse width as a function of distance. Right: Output power as a function of distance.

The comparison of the four graphs is shown in Fig. 4.21

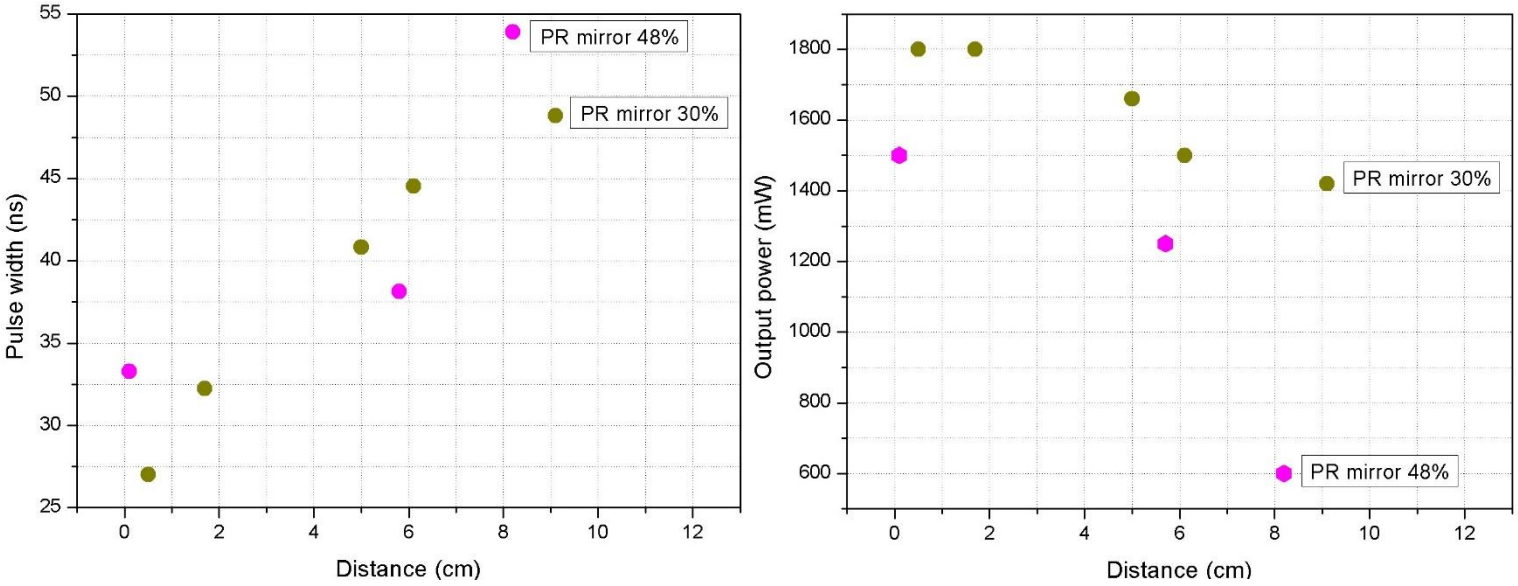

Figure 4.21. Pulse width as a function of distance (left) and output power as a function of distance (right) for the self-seeding cavity with 30% and 48% reflectivity, respectively.

The partially reflecting mirror does not affect the pulse width. However, the distance between the output coupler and partially reflecting mirror is sensitive. The pulse width is increased, while the distance is increased. This happens due to the cavity becomes larger.

5. Atomic beam spectroscopy of Ag

In this part of the project, the combination between the self-seeded grating-based Ti:sapphire laser and the existing three Ti:sapphire systems of laboratory (optical table 1 and 2, Chapter 3) are used for the saturation measurements and delay curve.

5.1. Motivation

The silver isotopes around the N = Z area have been of great interest for many years. A plenty of phenomena can occur by these isotopes because they are close to the N=Z line. For many reasons [18] the existence of the two-proton decay form of ^{94}Ag was disputed. In order to be resolved this problem, it is necessary to execute direct mass measurements ^{93}Pd, ^{94}Ag και ^{94m}Ag (21^{+}), Through this way, they will allow a clear determination of the isomer's energy.

5.2. Laser spectroscopy of silver

An efficiency laser ionization scheme for the silver has been characterized and tested (ref). It is a three steps ionization scheme. The final transition is non – resonant ionization.

The self-seeded grating-based Ti:sapphire laser is used in order to access AI (auto-ionization) state from the third level and improve the ionization efficiency. At the AI state, the cross section is bigger than the non – resonant ionization by factor of 100. Instead of being found the AI state, the Rydberg series is discovered starting from an unexpected state. It is not AI state because the AI states are not series and they are very broad.

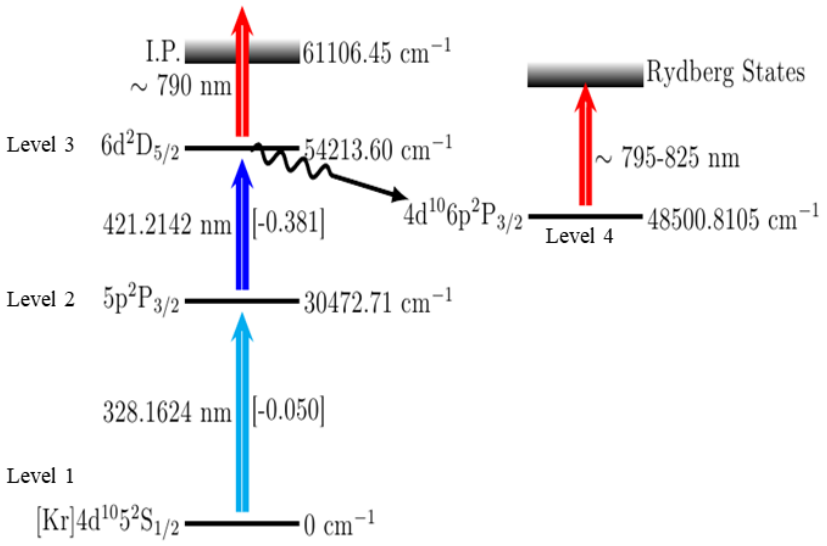

Figure 5.1. The resonance laser ionization scheme for silver and the silver Rydberg scheme.

The Rydberg series are observed in the ABU only when the intensity of the third step is low. If this happens, the transition from level three to level four is a weak path. Therefore, the transition from level three to level four is possible. Otherwise, if the intensity of the third level is not low, the non – resonant ionization covers the effect.

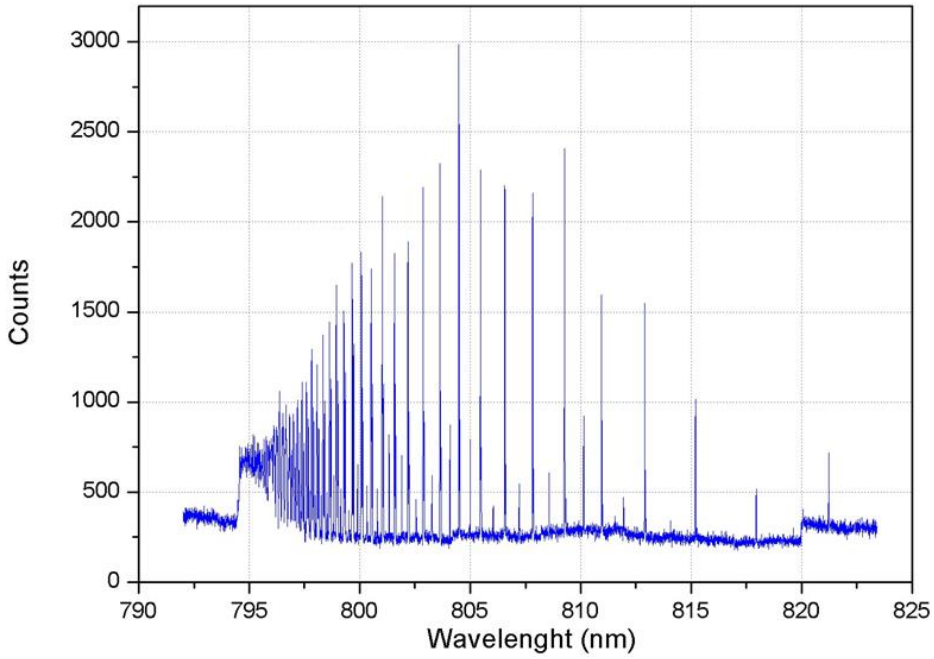

Figure 5.3. Results of Ag Rydberg scans.

5.3. Saturation curves

The aim for the saturation surves is to make a comparative assessment of the ionization efficiency by comparing the ionization rate of a Rydberg peak and the ground level between the peaks. Furthermore, the efficiency is demonstrated by comparing the Rydberg series.

In order to create the saturation curves the two lasers overlap. To fit the data, it is used the eq. 2.19, where for simplicity in this eq. assuming δ=0, and it becomes:

$$p = A\frac{\frac{I}{I_{sat}}}{(1+\frac{I}{I_{sat}})} \qquad 5.1$$

However, it is not used the I and I_{sat} due to non-measurement of the spot size of the laser beam during the experiment. Thus, it is used the P and P_{sat}, which are the output power and the equation 5.1 becomes:

$$p = A\frac{\frac{P}{P_{sat}}}{(1+\frac{P}{P_{sat}})} \qquad 5.2$$

Thus, based on the above mentioned, the following saturation curves are created for a specific value of wavelengths. For each wavelength, the deflector is set first on 0 and after on 200 V.

Wavelength: 792.943 nm

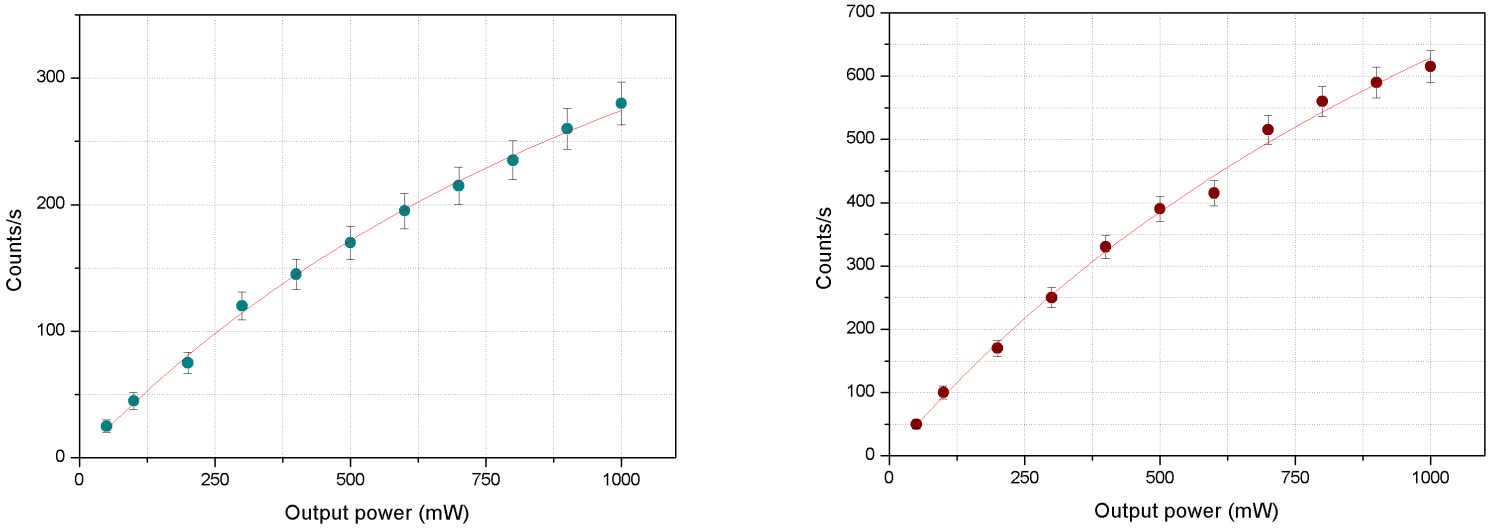

Figure 5.4. Left panel: Saturation curve for 0V. Right panel: Saturation curve for 200V.

Wavelength: 794.003 nm

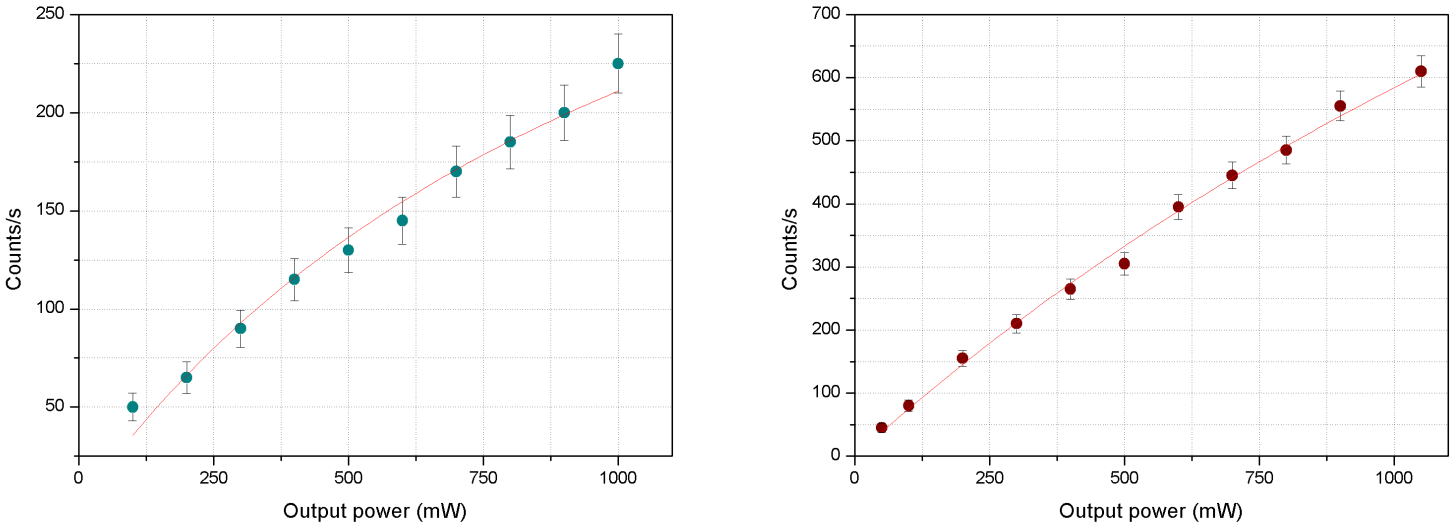

Figure 5.5. Left panel: Saturation curve for 0V. Right panel: Saturation curve for 200V.

Wavelength: 803.6347 nm

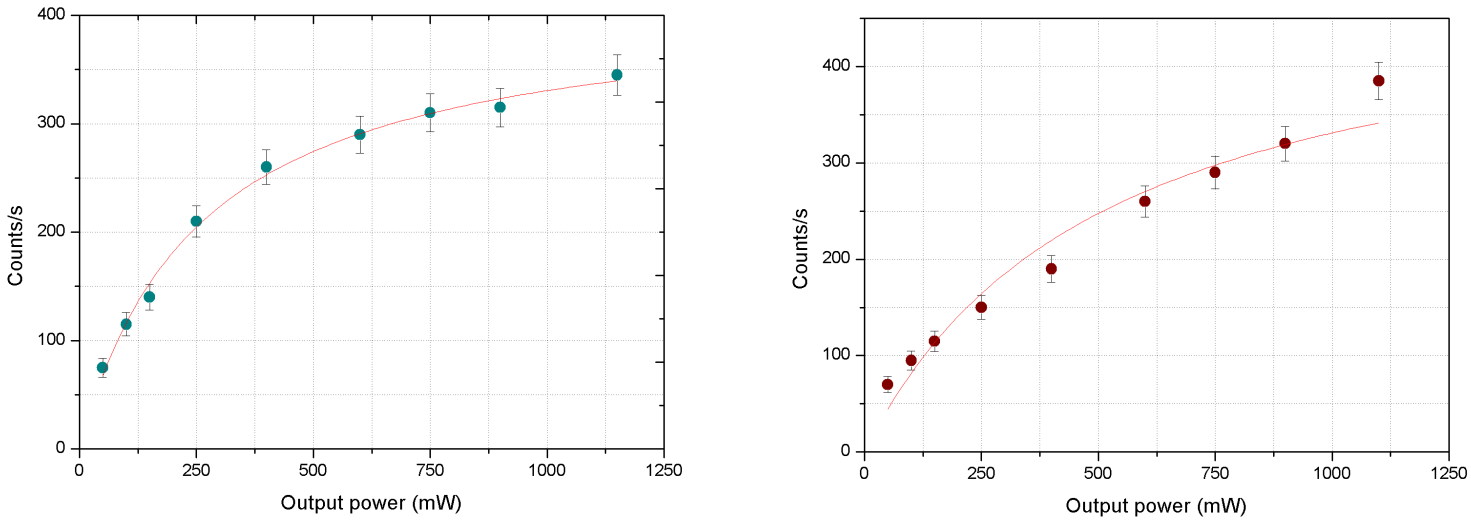

Figure 5.6. Left panel: Saturation curve for 0V. Right panel: Saturation curve for 200V.

Wavelength: 804.4869 nm

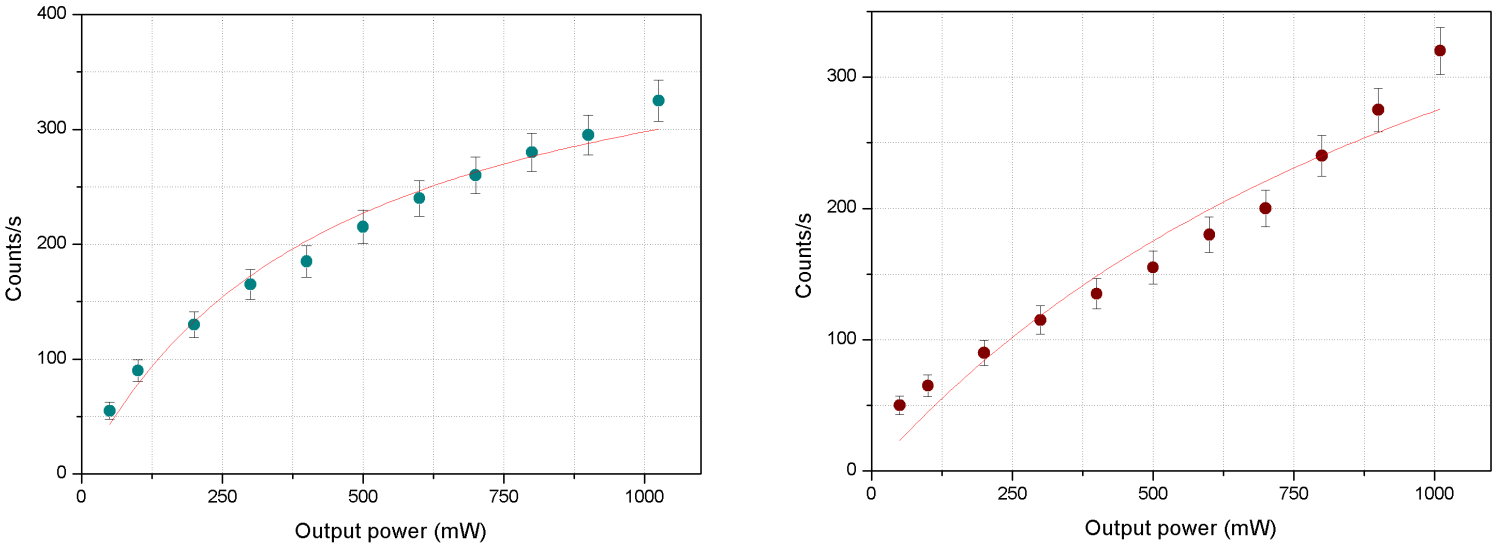

Figure 5.7. Left panel: Saturation curve for 0V. Right panel: Saturation curve for 200V.

Wavelength: 805.4616 nm

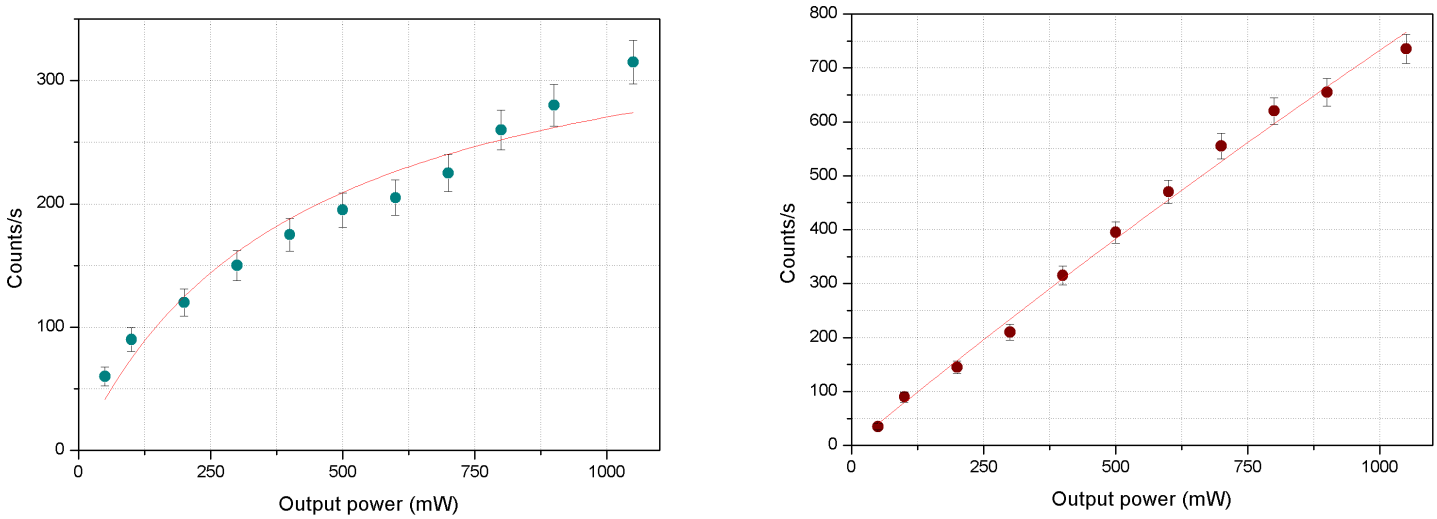

Figure 5.8. Left panel: Saturation curve for 0V. Right panel: Saturation curve for 200V.

Wavelength: 821.2284 nm

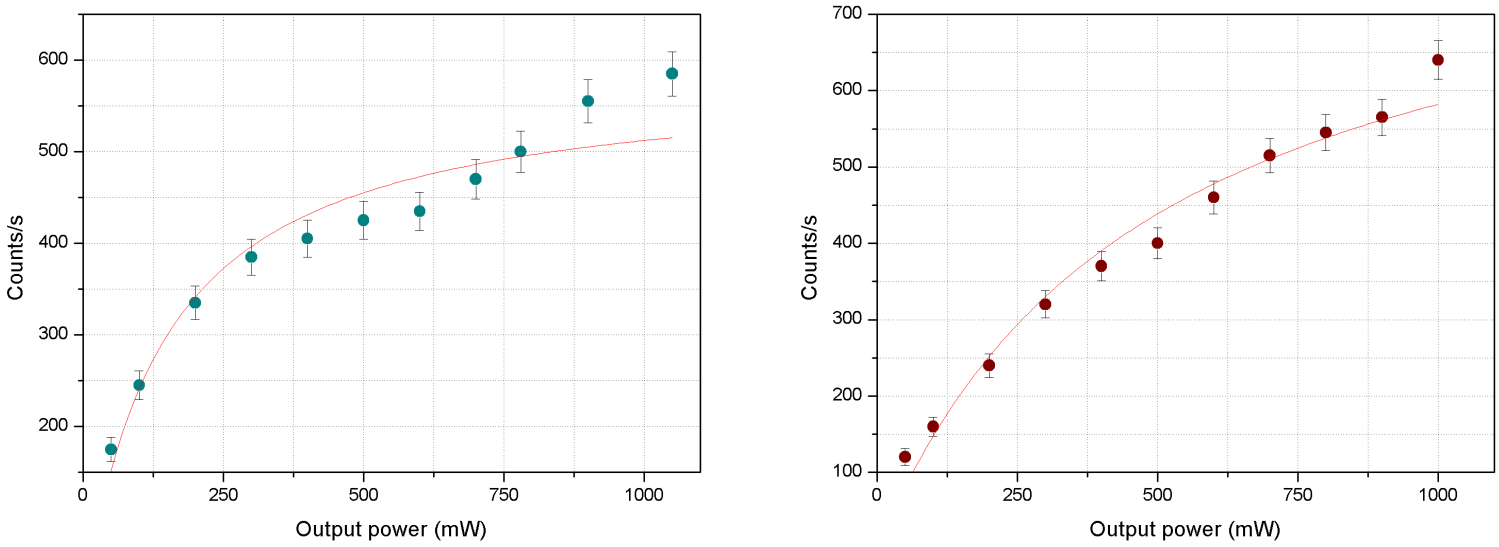

Figure 5.9. Left panel: Saturation curve for 0V. Right panel: Saturation curve for 200V.

Wavelength: 822.7228 nm

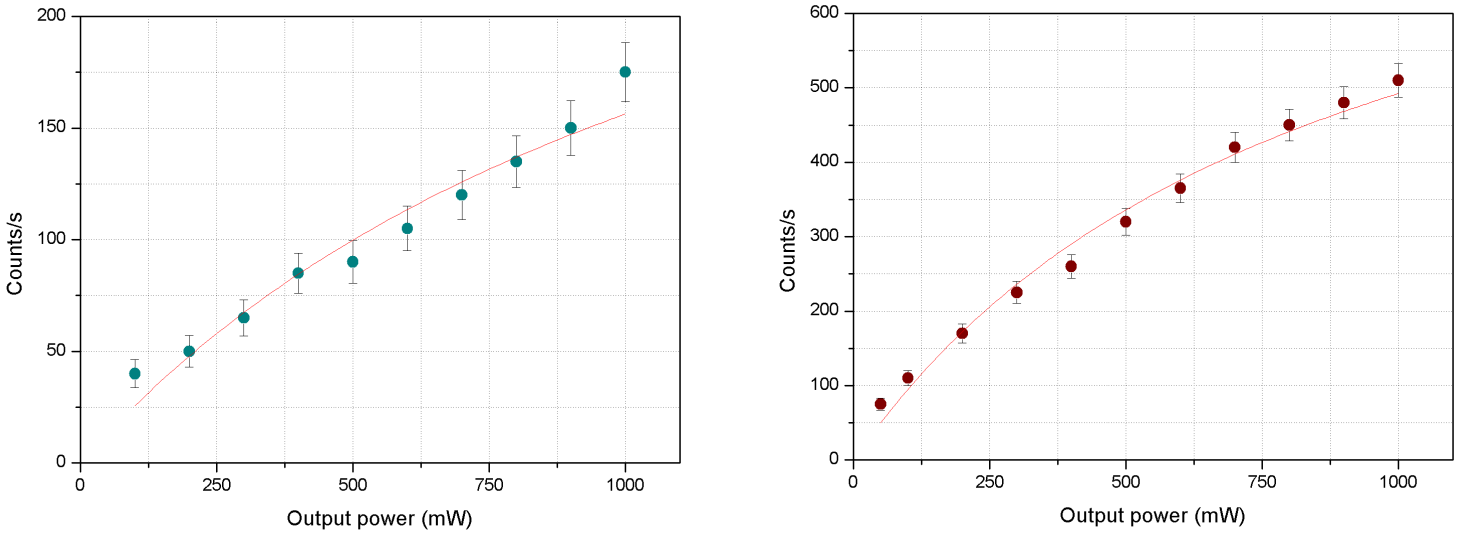

Figure 5.10. Left panel: Saturation curve for 0V. Right panel: Saturation curve for 200V.

Analyzing further the figure 5.3 between the region 792 – 796 nm of the Rydberg scan, it is observed that counts are not fully saturated even at high energies. That means that the output power can increases more. In addition, it means that it is about a non – resonant transition. In the same time, in the middle of the Rydberg scan (802 – 806 nm), counts are fully saturated, so Rydberg series appeared.

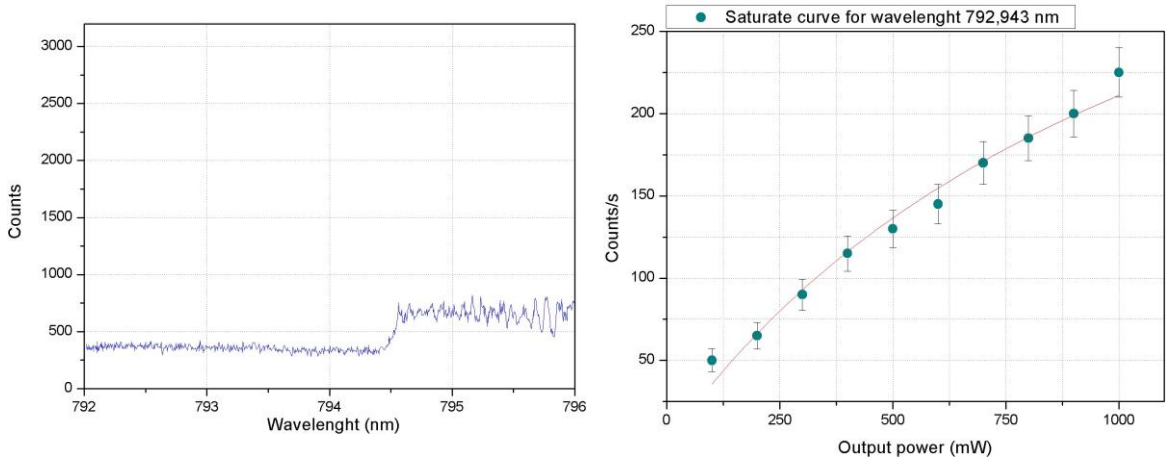

Figure 5.11. Region between 792 – 796 nm: The left panel shows the ion count rate vs. wavelength. The right panel of the figure illustrates the ion count rate vs. laser power.

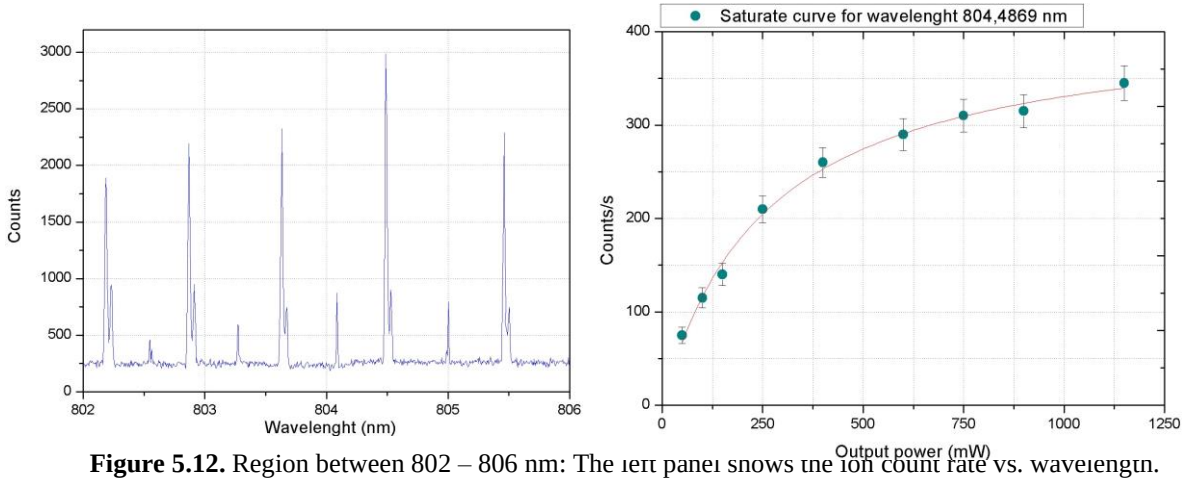

Figure 5.12. Region between 802 – 806 nm: The left panel shows the ion count rate vs. wavelength. The right panel of the figure illustrates the ion count rate vs. laser power.

5.4. Delay curve

In this section, the lifetime of level four of figure 5.4 is calculated. In order to create the delay curve, it is necessary to delay the infrared laser. So, for many delays, the time and the counts are estimated.

To fit the curve, a similar to the exponential decay equation, is used. The equation is the following, where τ is the lifetime.

$$y = Aexp(-\frac{x}{\tau}), \tag{5.3}$$

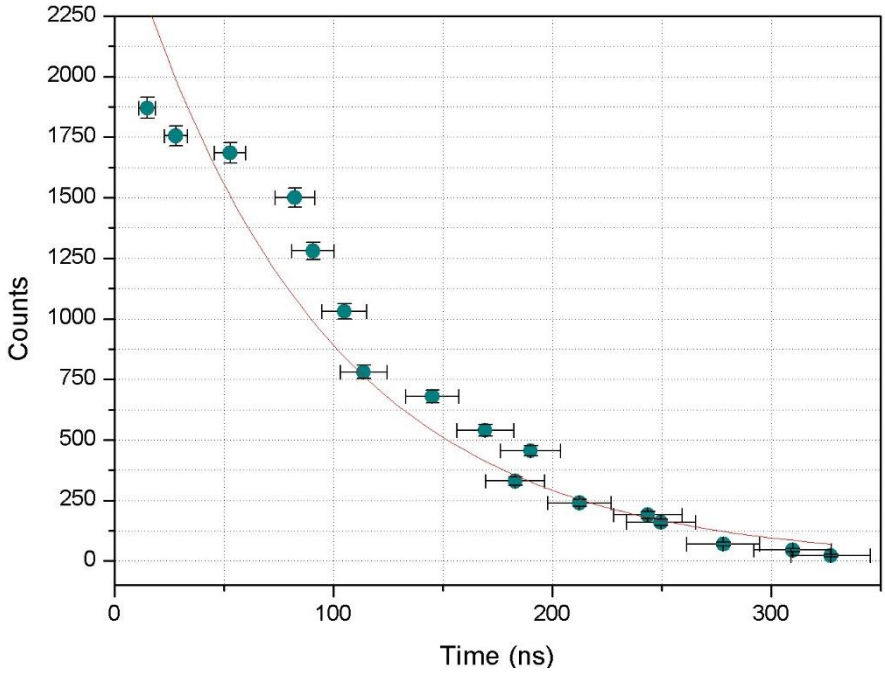

Figure 5.12. Probing the level lifetime of the fourth level

From the Fig. 5.12, the silver's lifetime at the level four is calculated. The Ag relaxes at this level and the lifetime is $\tau \sim 90ns$.

6. Summary and Outlook

The self-seeded grating-based Ti:sapphire laser is an important technical development and an useful tool. Using mirror with a 48% reflectivity provides the highest output power improvement compared to the non – seeded resonator. In addition the mirrors with a reflectivity 70% and 80% showed no additional seeding effects. It is worth to note that the partially reflecting mirror does not affect the pulse width. However, the distance between the output coupler and partially reflecting mirror is sensitive. The pulse width is increased, while the distance is increased. This happens due to the cavity becomes larger. In the future, a mirror with reflectivity of between 55% and 65% will be tested to see where the limit for the seeding effects is still visible. Intra – cavity second harmonic generation will be a future goal. To realize that o frequency – doubling crystal will be inserted between the output coupler and the first curved mirror.

As regards the second part of the thesis, the self-seeded grating-based Ti:sapphire laser has already used for the search of auto-ionization states of silver and the Rydberg series discovered. The data is under analysis. At delay curve, the silver's lifetime at the level four is calculated. This value is close that the reference expects to find [19]. However, it is important and necessary to investigate more in the future. In the future, the laser will be used for the search of atomic states on different elements.

References

1. V. N. Fedosseev, Yu. Kudryavtsev, and V. I. Mishin. *Resonance laser ionization of atoms for nuclear physics*. Physica Scripta, 85(5):058104, 2012.
2. V. T. Sonnenschein. *Laser developments and high resolution resonance ionization spectroscopy of actinide elements*. PhD thesis, University of Jyväskylä, 2015.
3. R. Li, J. Lassen, S. Rothe, A. Teigelhofer, and M. Mostamand. *Continuously tunable pulsed Ti:Sa laser self-seeded by an extended grating cavity*. Optics Express, 25(2), 1123, 2017.
4. E. P. Benis. Lecture notes from course: *Φυσική των Laser*. University of Ioannina (UOI), 2013.
5. O. Svelto. *Principles of Lasers*. 5th edition, Springer, 2009.
6. M. Reponen. *Resonance laser ionization developments for IGISOL-4*. PhD thesis, University of Jyväskylä, 2012.
7. H.D. Young and R.A. Freedman. *University physics with modern physics*. 11th edition, Pearson Education, 2004
8. E. Loewen and C. Palmer. *Diffraction grating handbook*. 6th edition, Newport Corporation, 2005.
9. S. Kouris. *Φυσική των Λέιζερ*. ISBN: 978-960-603-232-5, 2015.
10. I.D. Moore. Lecture notes from course: *FYSN552- Lasers and traps in nuclear physics*. University of Jyväskylä, 2017.
11. H. J. Kluge. *Resonance ionization spectroscopy and its application*. Acta physica polonica, 86(1-2), 1994.
12. T. Kessler. *Development and application of laser technologies at radioactive ion beam facilities*. PhD thesis, University of Jyväskylä, 2008.
13. I. Pohjalainen. *Gas-phase chemistry, recoil source characterization and in-gas-cell resonance laser ionization of actinides at IGISOL*. PhD thesis, University of Jyväskylä, 2018.
14. R. E. Horn. *Aufbau eines Systems gepulster, abstimmbarer Festkörperlaser zum Einsatz in der Resonanzionisations-Massenspektrometrie*. PhD thesis, University of Mainz, 2003.
15. RP Photonics. https://www.rp-photonics.com/.
16. Thorlabs. https://www.thorlabs.com/.
17. Ortec. https://www.ortec-online.com/.
18. B. Blank and M. Ploszajczak. Reports on Progress in Physics 71, 046301, 2008.
19. T. Badr, M. D. Plimmer, P. Juncar, M. E. Himbert, Y. Louyer and D. J. E. Knight. *Observation by two-photon laser spectroscopy of the* $4d^{10}5s\ ^2S_{1/2} \rightarrow 4d^9 5s^2\ ^2D_{5/2}$ *clock transition in atomic silver*. Physical review A 74, 062509, 2006.
20. P. F. Moulton, *Journal of the Optical Society of America* B 3, 1, 125, 1986.
21. J. E. Geusic, H. M. Marcos, L. G. V. Uitert, *Applied Physics Letters* 4, 10, 182, 1964.
22. W. T. Silfvast, *Laser Fundamentals*, Cambridge University Press, 1996.